Abstract

RAMIREZ VICENS, MAGALY ALEXANDRA. Cellulose Nanocrystals Reinforced Electrospun Poly(lactic acid) Fibers as Potential Scaffold for Bone Tissue Engineering. (Under the direction of Dr. Lucian A. Lucia and Dr. Elizabeth Loboa.)

Poly(lactic acid) / Cellulose Nanocrystals (PLA / CNs) were simultaneously electrospun to fabricate a novel renewable and biocompatible nanocomposite as potential scaffold for bone tissue engineering. CNs were successfully incorporated into the PLA fibers to reinforce the electrospun fiber mat. Thermal, chemical and mechanical analyses were performed to characterize and determine the properties of the scaffold fabricated. Highly porous fibers with fibers diameters in the range of 500-1000 nm were characterized by Scanning Electron Microscopy (SEM) and Transmission Electron Microscopy (TEM). Crystallinity of the electrospun nanocomposite was studied by Differential Scanning Calorimetry. Adipose-derived human mesenchymal stem cells (hMSCs) were used to study the cytocompatibility of the nanocomposite scaffold. Life/dead cell assay was performed to determine cell viability of the scaffolds. After one week of cell culture, confocal microscopy indicated that the cells grown on the PLA / CNs nanocomposite were confluent and very well aligned along the fibers while cells cultured on pure PLA fibers were not as confluent as in the developed nanocomposite. This project has demonstrated the feasibility of the fabricated PLA/CNs nanocomposite as a potential scaffold for bone tissue engineering.

Cellulose Nanocrystals Reinforced Electrospun Poly(lactic acid) Fibers as Potential Scaffold for Bone Tissue Engineering

by
Magaly Alexandra Ramírez Vicéns

A thesis submitted to the Graduate Faculty of
North Carolina State University
in partial fulfillment of the
requirements for the Degree of
Master of Science

Forest Biomaterials

Raleigh, North Carolina

2010

APPROVED BY:

_____	_____
Dr. Elizabeth Loboa	Dr. Orlando Rojas
Co-chair of Advisory Committee	Member of Advisory Committee

_____
Dr. Lucian Lucia
Chair of Advisory Committee

DEDICATORIA

A mi madre por todo su sacrificio, apoyo y amor incondicional. Gracias por haber sido guía a través del enigmático sendero de la vida, pero sobretodo gracias por dejarme ir, crecer, tomar riesgos y descubrir. Sin duda alguna, eres ejemplo de superación y admiración para muchos, pero para mí siempre has sido y serás valentía e inspiración. Agradezco a Dios por haber sido tú la escogida a ser mi madre…nadie pudo haberlo hecho mejor.

DEDICATION

To my mother for all her sacrifice, support and unconditional love. Thanks for being my guidance through the path of life, but above all, thanks for letting me go, grow, take risks and discover. You are a model of encouragement and admiration for some people, but to me you have always been and will always be inspiration. I thank God for choosing you as my mom…nobody could have ever done it better.

BIOGRAPHY

Magaly A. Ramírez Vicéns was born on August 9, 1985 in Caguas, Puerto Rico to Magaly Vicéns and Angel Ramírez. While spending her childhood taking modeling classes and dreaming about becoming a lawyer in the future, she suddenly changed her mind and decided to be a Chemist. In 2003, she graduated from Cristo de los Milagros Academy and enrolled into the Chemistry Program at the University of Puerto Rico at Cayey. While struggling with Chemistry classes she also participated in many organizations such as the Chemistry Club and the RISE (Research Initiative for Scientific Enhancement) Program. In her sophomore year she received an invitation letter to participate in many summer research program interviews taking place at school. As a result of this, she participated in summer internship programs at University of Pennsylvania and North Carolina State University. Motivated by many research opportunities, great academic environment, she decided to leave the beautiful island she belongs to and pursue a graduate degree at North Carolina State University. In spring of 2008, Magaly began her Master of Science degree at the Department of Forest Biomaterials under the tutelage of Dr. Lucian Lucia and Dr. Elizabeth Loboa.

ACKNOWLEDGEMENTS

I would like to thank my advisor Dr. Lucian Lucia and also Dr. Xiaodong Cao for all the support and guidance towards the completion of this project. Thanks to the members of my committee Dr. Elizabeth Loboa and Dr. Orlando Rojas for their support and the acceptance of this project.

Thanks to my mom Magaly Vicens, my sister Tania Ramirez, and all family members for their love and support.

Thanks to all my volleyball teammates!...great times at the volleyball court laughing and having fun together! Last but not least I would like to thank my roommate and friend Keren Cepero for all her support, advice and, of course, all her delicious cooking.

TABLE OF CONTENTS

LIST OF TABLES

LIST OF FIGURES

Chapter 1

Introduction

1.1 Tissue engineering

Tissue engineering has been defined as “the application of the principles and methods of engineering and the life sciences toward the fundamental understanding of structure-function relationships in normal and pathological mammalian tissues and the development of biological substitutes that restore, maintain, or improve tissue function”[1]. This area aims to combine cells, scaffold materials, and bioactive peptides to guide the repair of tissue formation [1]. The main approach in tissue engineering is to harvest a small biopsy of cells from the patient’s body, seed them on a scaffold to culture the desired tissue, and transplant the tissue back into the patient. In order to satisfy these criteria it is important to consider three key factors: cells, scaffold, and cell matrix (scaffold) interaction [2].

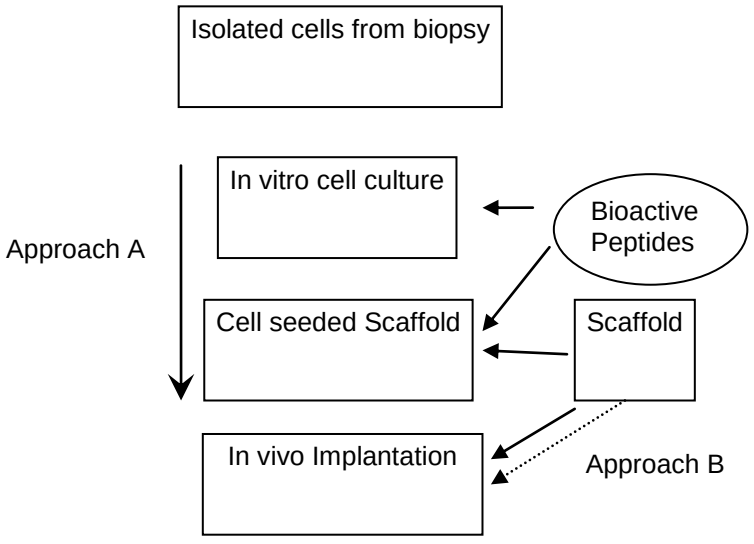

Figure 1. Principle of tissue engineering. Tissue engineering approaches in regeneration of tissue or organ [1]

Literature Review

1.2 Type of cells and cell-scaffold interaction

Cells are the basic units of a living organism and also an important factor in the success of bone tissue engineering. These units are usually categorized as stem cells (Figure 2), which are defined as unspecialized cells, and non-stem cells, which are specialized cells.

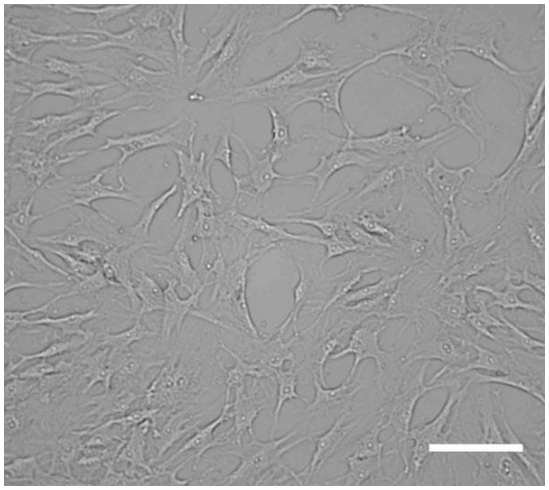

Figure 2. Human Mesenchymal Stem Cells [3]

Stem cells have attracted the attention of tissue engineers due to the fact these are able to divide but not to differentiate, whereas non-stem cells are committed to form specific types of cells [2]. Stem cells can be categorized as embryonic or adult cells [2, 3]. Embryonic stem cells are derived from the early stage of an embryo and are usually found in the inner cell mass of the pre-implantation embryo, at the blastocyst stage [2, 3]. These types have more potential than adult stem cells, but are less used in tissue engineering due to several ethical and legal controversies concerning their use for humans [2]. Adult stem cells are typically found in the bone marrow as hematopoietic stem cells (HSCs), which are responsible for the formation of blood cells, and mesenchymal stem cells (MSCs),

which are responsible for the formation of bone cells [2]. Mesenchymal stem cells were firstly described by Friedstein and since then they have been studied for many decades in bone tissue engineering [4, 5-6]. Biocompatibility of a tissue scaffold relies on their non-toxic properties and cell-scaffold molecular interaction.

By definition, a scaffold is a temporary supporting structure for growing cells and tissues [4]. A scaffold should have specific properties to work as a substitute for the extracellular matrix, which is a network found in the extracellular space that promotes cellular proliferation and provides support to cells. Some ideal properties that a scaffold should have are biocompatibility, three-dimensionality, porosity (> 90%), high surface area, biodegradability, and good mechanical properties [1]. The fabrication of scaffolds with properties similar to those of the extracellular matrix (ECM) has always been a challenge in tissue engineering. The ECM is a porous nano-fibrous environment in the body that provides support to the cells and promotes guiding and proliferation [2].

1.3 Current challenges and efforts in Tissue Engineering

One of the biggest challenges that are currently faced in tissue engineering is the manipulation of processing methods and composition of materials in order to develop scaffolds with controlled degradation rate, high porosity, orientation, high surface area, good mechanical properties, as well as cytocompatibility. The control of the degradation rate of a scaffold is one of the main focuses in tissue engineering. The scaffold should not degrade faster than the regeneration of tissue to give enough support to the tissue being formed but it should not either degrade slower, since it would hinder the tissue being

regenerated. By copolymerization it is possible to change the degradation behavior of polymers. It has been reported in the literature that polyurethanes degradation can be modified by copolymerizing with polyethylene-propylene-polyethylene tri-block co-polymer and poly(ε-caprolactone). Increasing the molar ratio of hydrophilic to hydrophobic segments increased the rate of degradation in vitro due to a higher water uptake and faster reduction in molecular weight [7]. Xin et al. also discovered that increasing the amount of borate content in bioactive glass scaffolds increased the degradation rate but also increased the cytotoxicity of the scaffolds [8].

The porosity of a scaffold is of high importance, especially in bone tissue engineering (Figure 3). Usually high porosity, between 70 to 90% allows a successful tissue in growth [9-13].

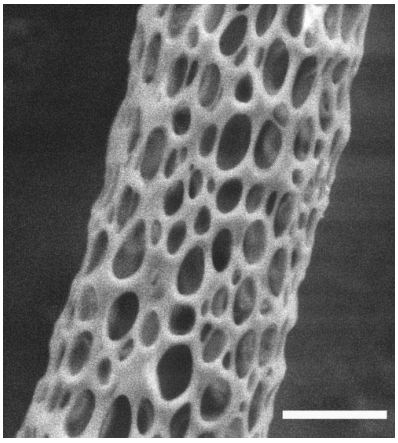

Figure 3. Highly porous polylactide nanofibers produced by electrospinning [14]

However, there is a debate of whether or not higher porosities could induce a reduction in mechanical strength of a scaffold [10]. Orientation of the scaffold matrix is another important factor in order to fully achieve physiological functions of natural and

engineered tissue [11-12]. Sun et al., 2006 findings show that fibroblasts are able to orient in a collagen scaffold applying an electrical stimulus. However, they also found that rat MSCs exhibit resistance to orientation under electrical stimulus. An alternate processing method to orient the scaffold matrix is the use of the electrospinning. This process has successfully produced orientation of scaffolds by using a rotating drum as fiber collector, which eventually induces cell alignment (Figure 4). However, there is no report of rotating drum ideal speed in order to produce the alignment of the fibers.

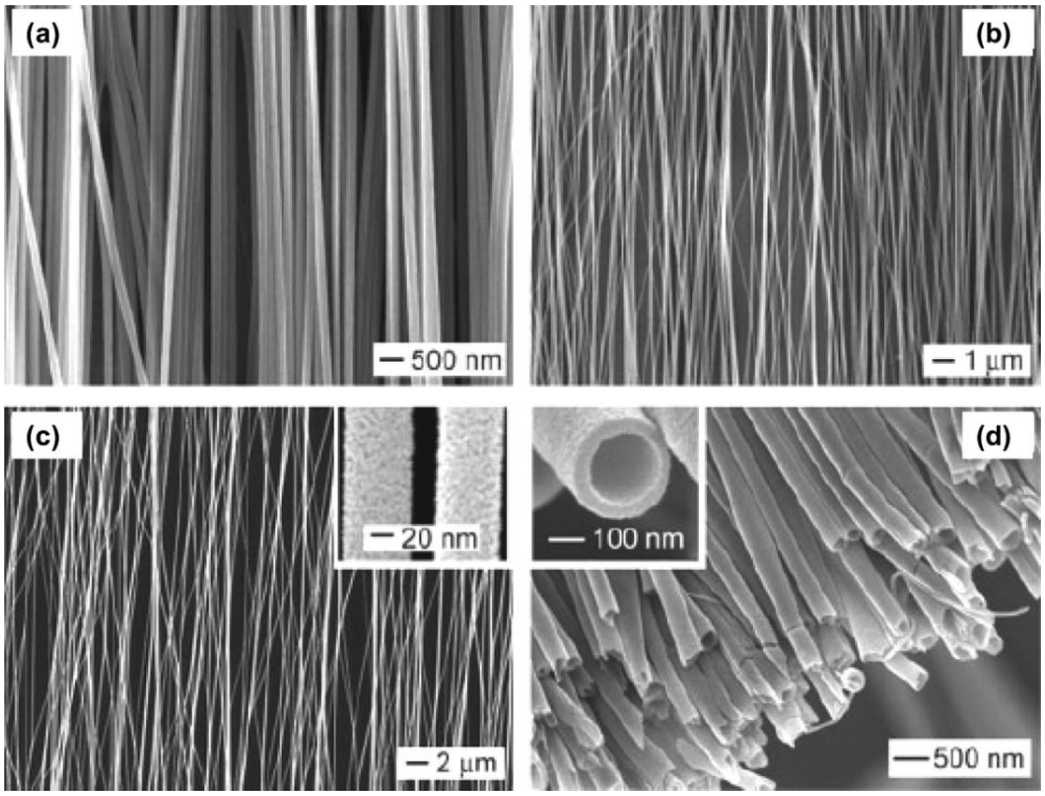

Figure 4. SEM micrographs of uniaxially aligned (A) single-phase nanofibers (carbon), (B) composite nanofibers (TiO2/PVP), (C) ionicdoped nanofibers (Sb-doped SnO2), and (D) nanotubes (anatase) [2]

The improvement of processing methods and techniques to achieve the ideal properties of a scaffold are a useful approach in tissue engineering. There are a few processes that can

be used for scaffold fabrication such as self-assembly, phase separation, solvent casting, and electrospinning [2, 15].

Self assembly is a process in which atoms and molecules arrange themselves into an ordered structure by non-covalent bonding (hydrogen bonding, ionic bonding, water-mediated hydrogen bonding, hydrophilic interaction, van der Waals interaction). This process allows the fabrication of 3D nano-fibrous matrices that promotes cell proliferation. However, this is a very difficult process that is usually limited to a few polymers and is unable to produce matrixes with controlled orientation [2]. Phase separation is another useful and easy process that involves a variety of steps that lead to the formation of nano-fibrous foam-like structures. It can produce 3D structures with controlled porosity and mechanical properties, but it can not produce fibers with controlled orientation [2].

The use of the electrospinning process has shown to be a good method to fabricate polymeric nanofibrous scaffolds that could mimic the ECM [2] (Figure 5).

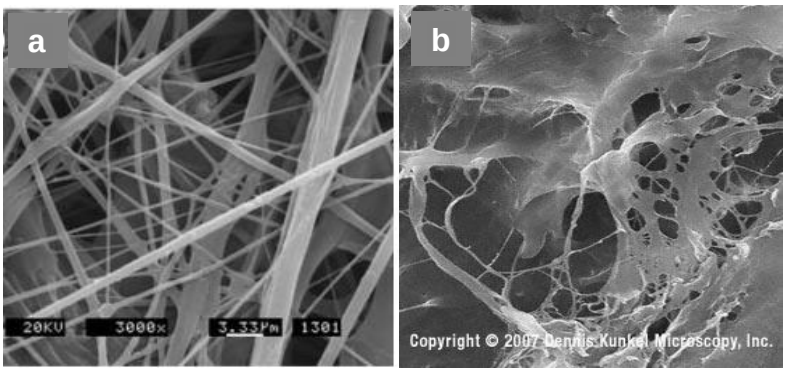

Figure 5. (a) Cellulose electrospun fibers [16]; (b) ECM structure [17]

A simple schematic of the electrospinning is shown in Figure 6. This process consists of a polymer solution that is injected in order to produce a jet of fibers that will eventually be collected into a grounded plate. What causes the generation of the electrically charged jet is the charge imbalance created by the voltage applied when it overcomes the surface tension of the polymer solution. The flow rate is usually controlled with a syringe pump.

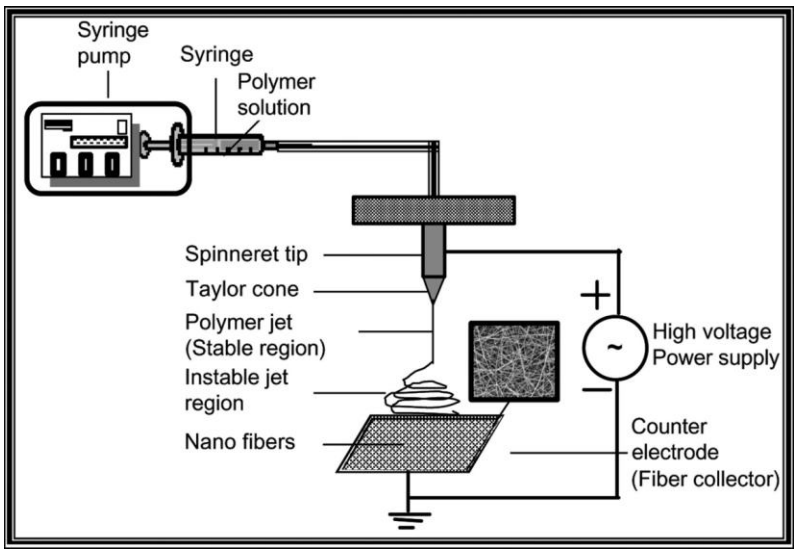

Figure 6. Schematic of electrospinning system [2]

The electrospinning process was first introduced by Zelency in 1914 [2] and since then it has offered many advantages in different areas of research such as textile and biomedical engineering. Other than being a simple and cost effective system, some of the advantages of this process are the fabrication of ultrafine fibers with high surface area, high aspect ratio, and controlled pore geometry [2].

It has been reported that the electrospinning can be used to produce fibers from a variety of polymers such as poly(ethylene oxide) (PEO), poly(vinyl alcohol) (PVA), poly(lactic acid) (PLA), poly(caprolactone) (PCL), as well as cellulose derivatives [18-24]. Highly

interconnected porous fibers of PLCL copolymers have been prepared by Kwon et al., 2005 using this process [25] (Figure 7). In addition to highly porous fibers, it has also been reported the feasibility of the electrospinning technique to produce fibers with small diameters and high surface area, which allows for a better cell migration and attachment [26] (Figure 8). Another advantage of using the electrospinning process is that it can be easily modified to improve morphology, composition and mechanical properties of the electrospun fibers.

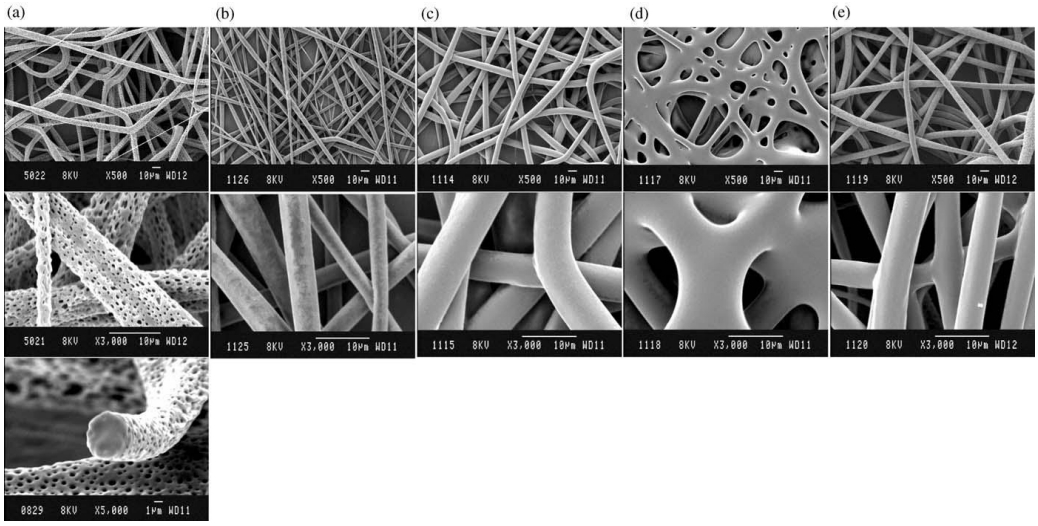

Figure 7. SEM images of electrospun microfiber fabrics made of PLCL (co) polymers:(a) PLL, (b) PLCL 70/30, (c) PLCL 50/50, (d) PLCL 30/70, and (e) PCL. [25]

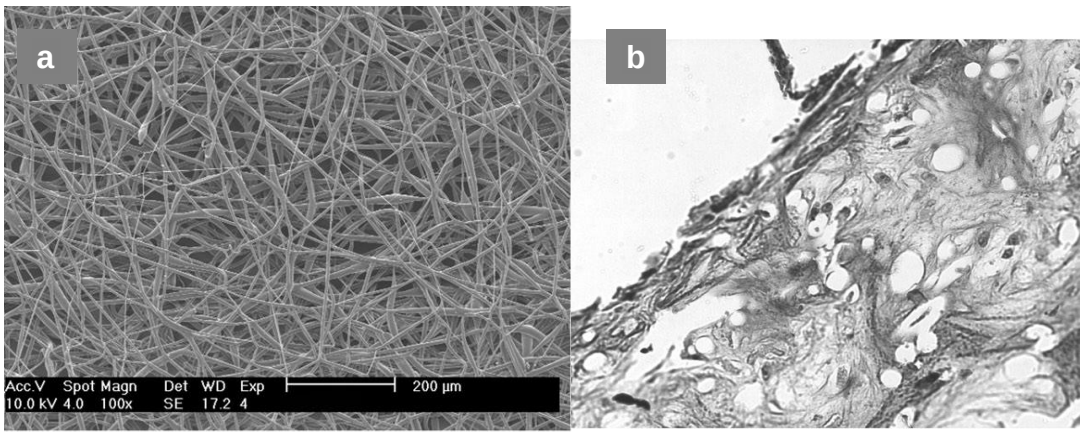

Figure 8. SEM micrographs of MSCs seeded on electrospun PCL scaffolds. (a) Scaffold prior to seeding. (b) After 4 weeks of culture, collagen type 1 is present in both the outer and inner parts of the scaffolds (immunostaining of type I collagen, _200). [26]

It has been reported that by increasing the flow rate of the solution, fibers diameter can be increased [27]. This behavior is ideal to a certain extent, especially in tissue engineering, since cells can accommodate better in the inside of the scaffold matrix [28]. The polymer solution composition and properties can also be modified in order to improve fiber morphology and mechanical properties. A decrease in the polymer concentration and an increase in electrical conductivity can produce smaller fiber diameters; however extremely low concentrations could promote the formation of beads instead of fibers [29-30]. It has been reported a decrease in fiber diameter by adding a salt to the polymeric solution (PEO). Salts increases charge density in the ejected jets and the repulsion due to an excess of charges under the electrical field, produce elongation forces that results in small diameter electrospun fibers [31]. Small fiber diameters increase surface area of the matrix; however producing very small diameters could also promote a decrease in pore size avoiding penetration of cells into the scaffold matrix.

The easiness in modification of the electrospinning apparatus is also an advantage.

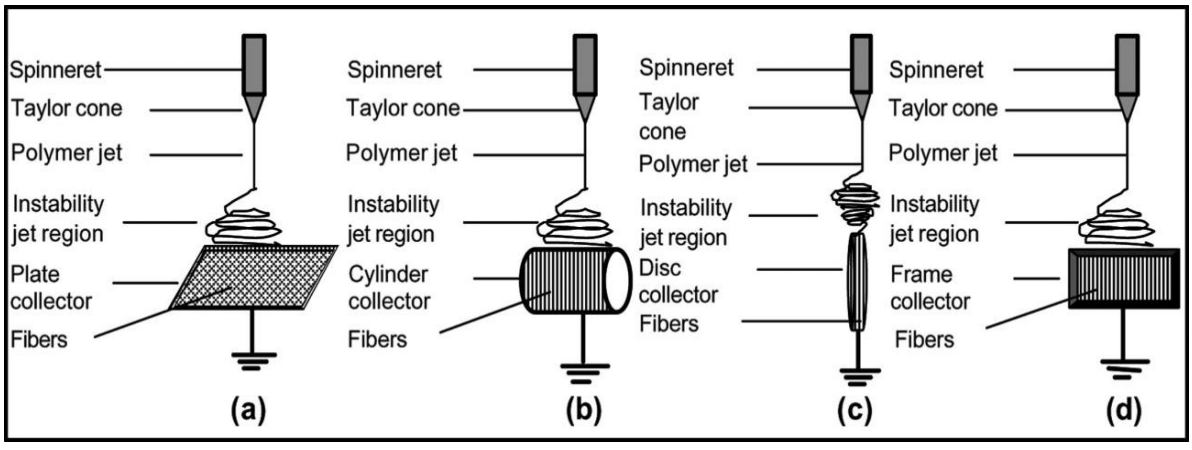

Figure 9. Types of nanofiber-collecting devices [2]

The type of collector plate can be changed in order to control fiber alignment [2] (Figure 9). The use of the conventional metallic static plate usually results in randomly oriented fiber mat while the rotating drum collector promotes fiber alignment. Core and shell method is also another way to modify the electrospinning apparatus structure in order to insert nanoparticles in the core of the electrospun fibers. This method has been successfully reported by Magalhaes et al., 2009 in the fabrication of cellulose nanocrystals reinforced fibers [32]. Due to the many scaffold processing advantages that the electrospinning offers, it has been extensively studied in the area of bone tissue reconstruction.

1.4 Bone tissue engineering (BTE)

Bone fracture is one of the most common events for clinical intervention in the United States. Replacement of osseous tissue has become an important area in tissue engineering. Bone is one of the most important structures in the body that plays several roles such as: protection of organs, support and attachment to muscles, generation of red and white blood cells for immunoprotection and oxygenation or other tissues, and, mineral storage and ion homeostasis [33]. It is composed of approximately 70% inorganic mineral and 30% of organic matrix mainly composed of collagen [34]. As seen in Figure 10, two types of bone make up the adult skeleton, cortical bone (~80%) and cancellous bone (~20%) [33]. Cortical bone comprises the outer shell of the bone structure; it provides mechanical stability and protection to vital organs having a porosity of ~10%, while cancellous provides a proper environment for metabolic activity having a porosity that ranges between 50-90% [33].

It is known that mineral content in the bone contributes to bone strength and mechanical properties; a variation of this inorganic content could potentially be the main reason for bone fracture. Although, collagen's role has been underappreciated for many years, it is believed that variations on its content in the bone, which may occur with age, could also be a cause for bone failure [35].

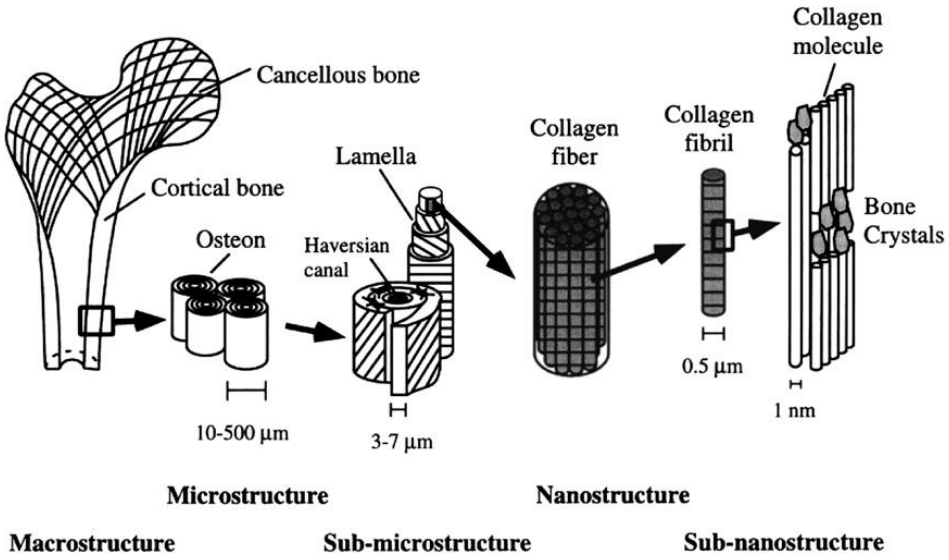

Figure 10. Hierarchical structure of bone at its various length scales [34]

This is a major event in older women, usually between the ages of 66 to 78 [35]. Whether or not one or the other is the main cause for bone fracture, bone deformation and fail to fracture always follows the same behavior. According to Figure 11 and 12, failure of bone is partitioned in three domains. In phase I, bone deforms reversibly with insignificant damage. In phase II, the material absorbs energy by developing microcraking damage at the expense of stiffness and residual strength. In phase III, energy is absorbed at and next to the final surface [36].

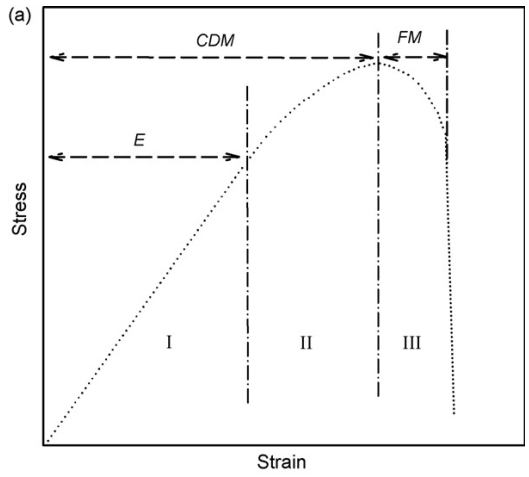

Figure 11. Stress/Strain behavior of bone to failure [36]

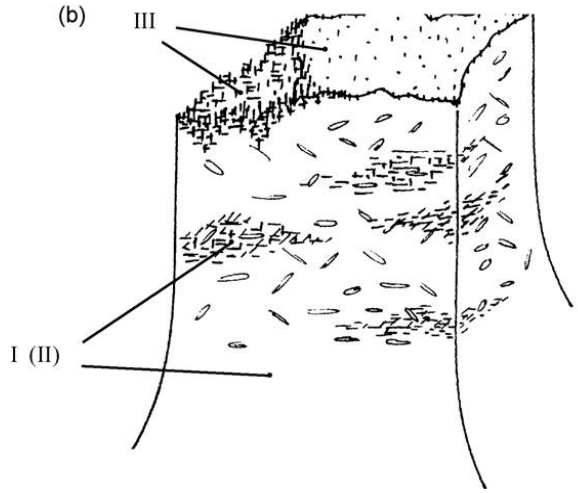

Figure 12. Bone structure while undergoing fracture [36]

The healing of a bone fracture stands on that the new bone is equivalent to the preexisting bone and no scar is formed. If a large portion of bone is lost due to injury, natural bridging will not bridge the gap [62]. Bone grafting has become second most common procedure in the United States with more than 500,000 procedures in order to repair bone fracture and defects in orthopaedics, neurosurgery and dentistry [37]. This is an

implantable procedure that replaces bone tissue with substitutes such as material from patient's own body, artificial, synthetic or natural materials.

Table 1. Common Orthopaedic Procedures Statistics Reported in 2006 [38]

Description	Number of Procedures	Women	Men	Mean Age
Total Knee Replacement	542	344	199	67
Total Hip Replacement	231	129	102	65
Spinal Fusion	349	188	161	53
Spinal Refusion	22	14	8	54
Procedures on Rotator Cuff Repair	20	10	10	----

The most common types of bone grafts are autografts, which in other words is bone taken from the same patient's body, and allografts, which is usually bone from another individual. There are three important processes in the success of bone regeneration, osteogenesis, osteoinduction and osteoconduction, along with the final interaction between host bone and grafting material which is called osteointegration [37] (Table 2).

Table 2. Autograft and allograft characteristics [37]

Bone graft	Structural strength	Osteoconduction	Osteoinduction	Osteogenesis
Autograft				
Cancellous	No	+++	+++	+++
Cortical	+++	++	++	++
Allograft				
Cancellous				
Frozen	No	++	+	No
Freeze-dried	No	++	+	No
Cortical				
Frozen	+++	+	No	No
Freeze-dried	+	+	No	No

Although bone grafts have been extensively used in medicine to repair bone defects, they have also shown some limitations such as inappropriate form, inadequate amount, risks of disease transmission, loss of biologic and mechanical properties, and increase in cost [39].

Due to previously mentioned limitations of autografts and allografts, the role of bone tissue engineering is to discover and develop biomaterials that could potentially restore, maintain or improve bone tissue function. One of the main challenges of this area is not just making these materials biocompatible or non-toxic, but also to develop materials that have specific mechanical properties that match those of bone tissue. The approximate elastic modulus of cortical bone is about 16-23 GPa, with a tensile strength of 80-150 MPa [34]. Cancellous bone has an elastic modulus of 12-900 MPa, and a tensile strength of 0.2-14 MPa [34].

1.5 Biomaterials in BTE: advantages and disadvantages

Synthetic implantable biomaterials such as metals, ceramics, and polymers offer many advantages over autografts and allografts for the treatment of bone defects [1]. However, the use of natural or renewable materials as scaffolds in tissue engineering have been a major focus since these materials have shown to be highly biocompatible, biodegradable, offer chemical functionality, and provide cheap and replenishing source of material [33].

More than two decades ago, a biomaterial was defined as a "systematically, pharmacologically inert substance designed for implantation within or incorporation within a living system" [34]. The main concept is that these materials act as scaffolds to

promote invasion of cells/tissue, growth, and guidance of tissue regeneration [40]. Biomaterials have been studied in depth for many years as substitutes for grafts in bone tissue engineering (BTE) due to their biocompatible and non-toxic properties. They also have found to be osteoconductive and osteoinductive, which means that they provide a passive porous scaffold to support or direct bone formation and also induce differentiation of stem cells into osteogenic cells [39] (Table 3).

There is a wide variety of biomaterials such as metals, ceramics, glass, composites and polymers that have been extensively used in BTE [41-47]. Calcium hydroxyapatite ceramics have been successfully used in bone tissue repair due to properties similarities to

Table 3. Osteoconductive scaffolds [37]

Type	Graft	Osteoconduction	Osteoinduction	Osteogenesis	Advantages
Bone	Autograft	3	2	2	"Gold standard"
	Allograft	3	1	0	Availability in many forms
Biomaterials	DBM	1	2	0	Supplies osteoinductive BMPs, bone graft extender
	Collagen	2	0	0	Good as delivery vehicle system
Ceramics	TCP, hydroxyapatite	1	0	0	Biocompatible
	Calcium phospate cement (CPC)	1	0	0	Some initial structural support
Composite grafts	β-TCP/BMA composite	3	2	2	Ample supply
	BMP/synthetic composite		3		Potentially limitless supply

Score: 0(none) to 3(excellent). DBM: demineralized bone matrix, TCP: tricalcium phosphate, BMA: bone marrow aspirate, BMP: bone morphogenetic protein

natural bone. However, the brittle nature of these materials does not match the fracture toughness of natural bone and there is a need turning them into composites in order to reinforce and improve their properties [42-44].

Metals have also been used for many decades in bone clinical interventions. Despite the fact that metals are strong, tough, and ductile, they are very susceptible to release toxic metallic ions and/or particles through corrosion or wear, which reduces biocompatibility [41]. Research attempts to improve biocompatibility such as combustion synthesis of Ti-Co alloys for orthopedic applications are currently under development [43]. However, many natural and synthetic polymers have attracted the attention of tissue engineers due to their tissue matching mechanical properties, biodegradability and also biocompatibility. Polylactic acid (PLA), Polycaprolactone (PCL), Hyaluronic acid (HA), starch, and collagen are some examples of polymers that have been extensively used in tissue engineering. Composites of these polymers with metals, ceramics as well as with some other types of biomaterials have also shown ideal properties in BTE. The aim of these composite materials development is usually to improve mechanical properties of the scaffold matrix as well as biocompatibility [45, 46].

1.6 Polymers

Degradable polymers have been used in medicine since the mid 20th century [40]. They have been studied since these can be used as implants without requiring a second surgical intervention for removal [48]. Polymeric scaffolds mechanical properties and chemical

behavior will mainly depend on molecular weight, crystallinity, thermal transition as well as degradation rate [40, 49].

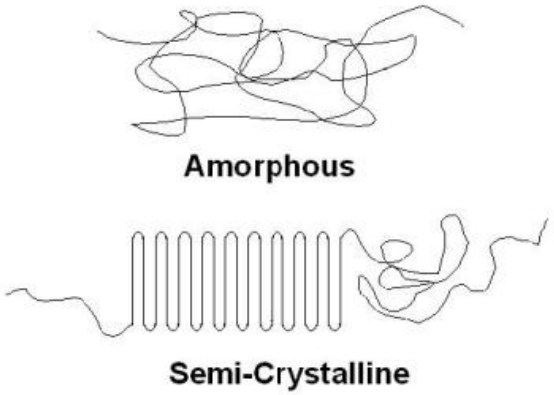

Figure 13. Amorphous and semi-crystalline polymers schematic representation [50]

Polymers are mainly divided into crystalline, semi-crystalline, and amorphous materials (Figure 13). However there is not such pure crystallinity for any polymer. Crystalline polymers are mainly composed by a crystalline and an amorphous domain. Crystalline domains in a polymer improve mechanical properties and also decrease total degradation time while the amorphous regions give to the polymer the ability to bend without breaking [40]. In other words, a balance between the amorphous and crystalline regions is desired in order to obtain ideal properties of the polymeric material. Semi-crystalline polymers exhibit high toughness at temperatures above the glass transition temperature (T_g) [51]. The T_g is defined as the onset temperature of main chain segmental motion allowing the chains to change conformation during load; below this temperature molecular motion ceases [40].

There are a variety of polymers such as poly (lactate acid), poly (glycolic acid) and poly (caprolactone) that have been successfully used in tissue engineering [28, 52] (Figure 14).

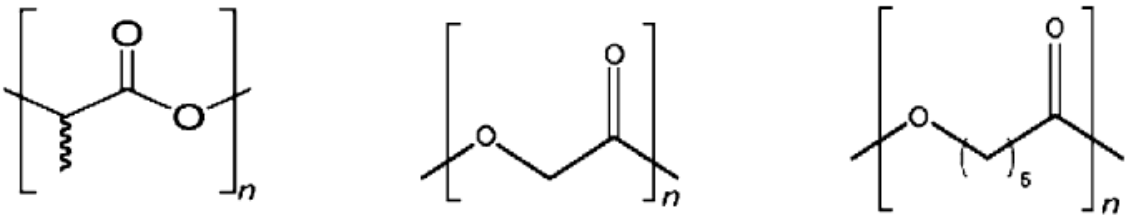

Poly (lactate acid) **Poly (glycolic acid)** **Poly (ε-caprolatone)**

Figure 14. Biodegradable polymers for bone tissue engineering [53]

However, co-polymerizing these polymers together or preparing composites out of them is usually an ideal method of taking advantage of the best properties of each individual polymer in order to improve polymeric matrix biological and mechanical properties [54-60]. In the following two sections of this literature review properties of polylactic acid and cellulose, as potential polymeric materials for bone tissue engineering, will be discussed.

1.6-1 Polylactic acid

For many decades, polylactic acid (PLA) has been used in medical applications, such as drug delivery systems, surgical implants and osteosynthetic devices [61]. This polymer can be produced by polymerization of lactic acid, via two different mechanisms: (1) Direct condensation and (2) formation of the cyclic dimer intermediate (lactide) (Figure 15). PLA biocompatibility and degradation properties are very well understood [7, 29, 52]. Its degradation is mainly influenced by four major factors: (1) the hydrolysis rate constant of the ester bond; (2) the diffusion coefficient of water in the polymer matrix; (3) the diffusion coefficient of the chain fragments within the polymeric matrix and (4) the solubility of the degradation product [7, 63]. Other than releasing non-cytotoxic

byproducts during degradation, PLA has some other advantages such as high crystallinity, which provides higher strength, glass transition temperatures (T_g) in the range of 60°C-70°C and melting (T_m) between 170°C-180°C [63-64] (Table 4). However, one of the most important advantages of PLA is that it can be easily tailored by material modifications [63]. One of the main approaches to improve its physical and chemical properties is by copolymerization [65-68], but PLA can also be electrospun in order to increase its surface area, porosity, permeability, as well as mechanical properties.

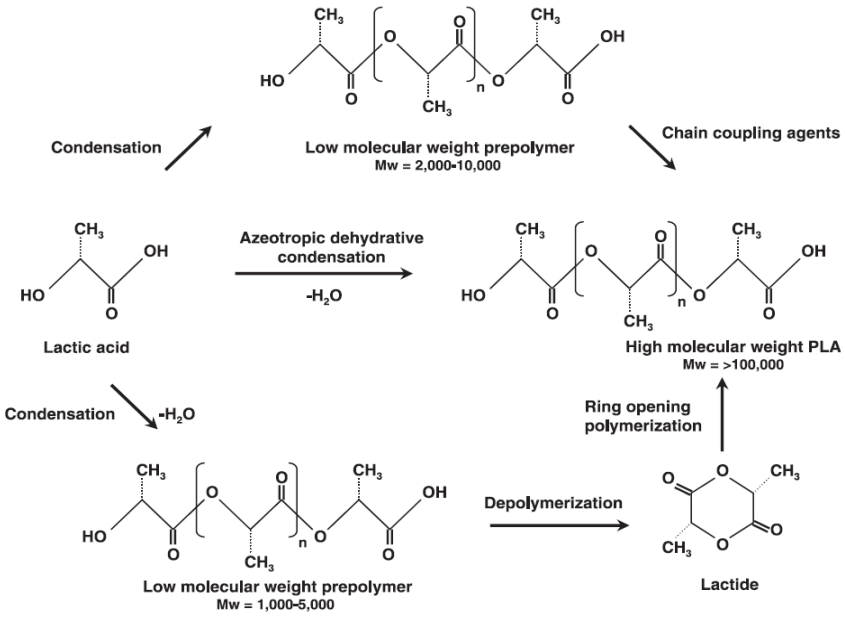

Figure 15. Synthesis of Poly(lactic acid) [63]

It has been reported that by electrospinning PLA it is possible to produce highly porous 3D structures that can act as cells scaffolds in BTE [56, 69-70]. Ultrafine PLA fibers in the nano-scale range can be produced in order to increase surface area of the material structure [22, 59-72]. Due to the great potential that PLA nano and micro fibers have in tissue engineering many research studies have focused on the modification of this matrix in order to improve cell response. Due to the hydrophobic nature of PLA, Kim et al., 2007

have been able to successfully incorporate gelatin into PLA matrixes in order to improve hydrophilicity and cellular affinity to scaffolds [73].

Table 4. Properties of PLA [63]

Property	Units	Condition	Value
Degree of crystallinity X_c	%	L-PLA	0-37
Density ρ	g/cm^3	Amorphous	1.248
		Single crystal	1.290
Heat of fusion ΔH_f	kJ/mol	L-PLA complete crystalline	146
		L-PLA fiber	
		As-extruded	2.5
		After hot drawing	6.4
Heat Capacity C_p	J/K/g	L-PLA with	
		M_v = 5300	0.60
		M_v = (0.2-6.91)x10^5	0.54
Glass transition temperature	K		326-337
Melting Point	K		418-459
Decomposition temperature	K		500-528
Swelling in water %		pH 7 buffer	2
Intrinsic viscosity (η) in chloroform at 25^{o}C	dl/g		3.8-8.2
Radiation Resistance	*G* value	Under nitrogen	
Co^{60} in benzene solution, 30^{o}C		Chain scission	26.5
		Cross linking	4.5
In water		Chain scission	
		Cross linking	23.0
IR peaks	cm^{-1}		
OH (alcohol/carboxylic)			3700-3450
-C=O			1750-1735
-COO			1600-1580
C-O			1200-1000
CH			950-700

Some other studies have mainly focused on the preparation of PLA fibers with the incorporation of nano-particles or compounds in order to have a better guidance of cells. For example, it has been possible to prepare electrospun hydroxyapatite (HA) / PLA

fibers, but it has also been possible to mineralize PLA scaffolds with HA by immersion of fibers in simulated body fluids [23, 56, 70]. The results showed that HA not only promoted the adhesion and proliferation of pre-osteoblast, but also increased the strength of the PLA fiber mat [23] (Table 5 and Figure 16).

Table 5. Electrospinning conditions for PLA/HA composite nanofibers and their corresponding physical and morphological characteristics [23]

Sample Code	Conditions				Properties				
	PLA:HA mass ratio [a)]	Voltage	Needle size	Spinning time	Tensile strength	Elongation	Young's modulus	Average pore diameter	Mean fiber diameter [b)]
		kV		h	MPa	%	Mpa	μm	nm
PLA	1:0	18-20	23 gauge	8	0.063 ± 0.004	27 ± 1.0	0.419 ± 0.013	4.51 ± 0.04	365 ± 83
PLA-HA1	1:0.05	18-20	23gauge	8	0.157 ± 0.005	30 ± 0.8	1.804 ± 0.026	1.32 ± 0.01	255 ± 45
PLA-HA2	1:0.2	18-20	23 gauge	8	0.262 ± 0.007	36 ± 0.9	4.711 ± 0.019	0.53 ± 0.03	135 ± 13

[a)]Concentration of 10 wt. -% PLA solutions in 2,2,2-trifluoroethanol; [b)]Mean diameter was calculated by measuring the size of 30 fibers with SEM

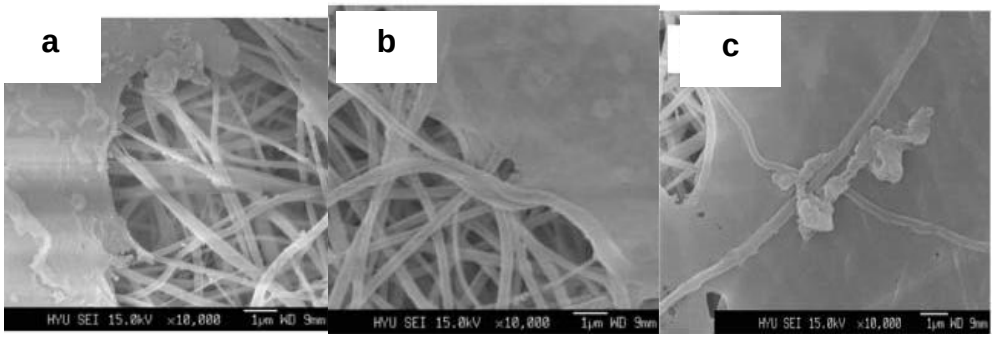

Figure 16. SEM images of cell/scaffold composites (PLA/HA) at (a) 7, (b) 14, and (c) 21 d of culture [23]

1.6-2 Cellulose Nanocrystals

Cellulose is one of the most abundant polymers on Earth. It can be found in all plants and it can also be produced by certain bacteria and sea animals [33]. Cellulose is a

polysaccharide mainly composed of cellobiose units linked together by β- 1,4- glycosidic linkages (Figure 17).

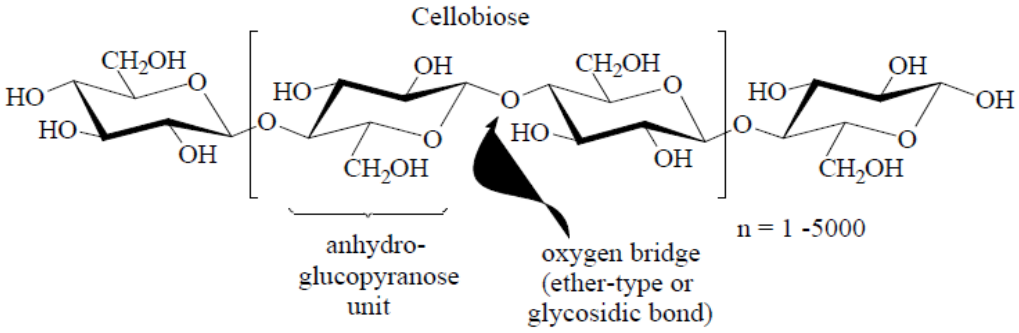

Figure 17. Chemical Structure of Cellulose

Various models have been proposed to explain the structure of cellulose in the plant cell wall. But the most accepted explanation is that due to the linearity of the cellulose backbone, chains form a framework of elementary microfibrils with crystalline and amorphous regions [74] (Figure 18). Owe to the high modulus of elasticity (MOE) of crystalline cellulose, calculated as 138 GPa, it has been exploited as a reinforcement agent for a variety of composites [32] (Table 6).

Table 6. Moduli of engineering materials compared to cellulose [32]

Material	Modulus (GPa)	Density (Mg m^{-3})	Specific Modulus (GPa Mg^{-1} m^3)	Reference
Aluminum	69	2.7	26	[279]
Steel	200	7.8	26	[279]
Glass	69	2.5	28	[279]
Crystalline cellulose	138	1.5	92	[10]

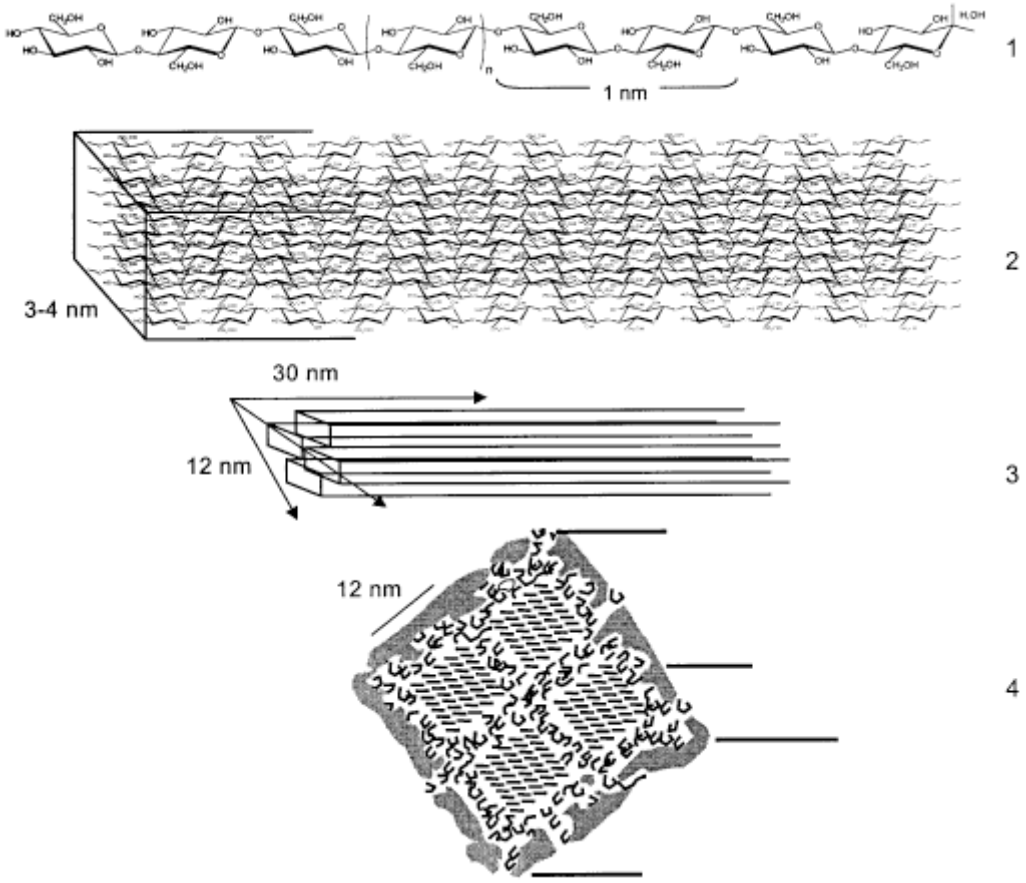

Figure 18. Chemical association in the plant cell wall: (1) the cellulose backbone, with an indication the length of its basic structural unit, cellobiose; (2) framework of cellulose chains in the elementary fibril; (3) cellulose crystallite; (4) microfibril cross section, showing strands of cellulose molecules embedded in a matrix of hemicelluloses and protolignin [74]

During acid hydrolysis the amorphous domains of the microfibrils are degraded, resulting in the preservation of crystallites which are called cellulose nanocrystals (CNs). The size of these nanocrystals varies depending upon the source from which they were obtained; but usually they are in the size range of 100-1000 nm in length and 3-50 nm in width [33]. The reinforcing ability of CNs lies in their high surface area and good mechanical properties [75-76]. CNs undergo strong interactions due to the resulting surface charges produced by the hydrolysis reaction and they have been reported difficult to disperse in

water [77-78]. It has been reported the feasibility of stabilize the suspension by chemically modifying the CNs and disperse them in organic solvents [79]. However, this modification usually affects the mechanical performances of the CNs by disrupting the three dimensional network of the nanocrystals [78]. In order to overcome this problem, it has been possible to disperse the CNs suspension in polar aprotic organic solvents, such as DMF and DMSO [78,80].

Cellulose nanocrystals have a broad variety of applications such as reinforcement agents for plastic composites, use in sensors, smart materials, membranes, textiles, electro-optic devices as well as biomedical purposes.

1.7 Overall Objective

Having in mind that cellulose has non-cytotoxic and biocompatible properties, the aim of this project is to make use of it as a renewable polymeric material in the preparation of a novel Cellulose Nanocrystals/Polylactic Acid (CNs/PLA) composite as a potential scaffold for BTE [81-82] . As previously mentioned, the electrospinning technique offers many advantages since the process can produce ultrafine fibers with high surface area, high aspect ratio, and controlled pore geometry. In order to enhance and control scaffold properties this technique has been employed in the preparation of CNs/PLA composite. Crystalline cellulosic biomaterials have high modulus of elasticity (MOE). We hypothesize that cellulose having a MOE of 138 GPa (cellulose type I) could improve the strength and mechanical properties of polymeric matrices. Therefore, due to the biodegradability and biocompatibility properties of PLA we intend to incorporate CNs on PLA electrospun fibers in order to enhance its mechanical properties.

Chapter 2

Experimental

2.1 Preparation of cellulose nanocrystals

Cellulose nanocrystals (CNs) were obtained by hydrolyzing cellulose from cotton. Sulfuric acid (H_2SO_4) 64% was added to cotton and stirred for 30 minutes at a temperature of 60^{o}C. The resulting CNs suspension was cooled down in an ice bath and centrifuged at a temperature of 10^{o}C and 10,000 RPM for about 30 minutes to remove acid content (supernatant). Deionized water was added and the suspension was centrifuged following the same conditions previously mentioned. The CNs suspension was dialyzed against tap water for a week; then it was dialyzed against deionized water for two more days. Deionized water was added to the suspension and centrifuged for 30 minutes at 10^{o}C and 5,000 RPM to precipitate the CNs. The supernatant was placed in 50 ml centrifuge tubes and added 10 ml of dimethylformamide (DMF). The suspension was centrifuged for 45 minutes at 10^{o}C and 12,000 RPM to exchange the solvent; added 10 ml of acetone to precipitate the CNs in suspension. DMF was added to remove acetone residues. This procedure was repeated 3 times. The final content of CNs in suspension was 3.5% wt (Figure 19).

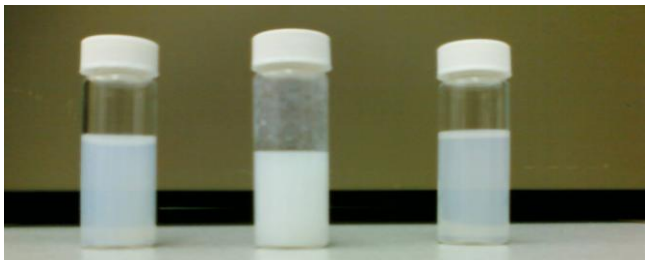

CNs Suspension in water | CNs Suspension in acetone | CNs Suspension in DMF

Figure 19. Cellulose Nanocrystals suspension after hydrolysis of cellulose with H_2SO_4

2.2 Preparation of PLA, PLA/CNs, PLA/CNs/HA blends

Seven different PLA/CNs blend solutions were prepared for this experiment. All solutions were 10% wt. PLA, but different CNs content. Three of the solutions contained 5% wt. hydroxyapatite (HA) content. The solvent system used for the preparation of all solutions was dichloromethane / DMF 3:1. A summary of the solution conditions is shown in Table 7.

Table 7. PLA, PLA/CNs and PLA/CNs/HA blend solutions conditions

Solution	PLA concentration (%wt.)	Ratio PLA/CNs/HA	Solvent System	Solvent System Ratio	Sonication time (h)
PLA	10%	Pure	dichloromethane/DMF	3:1	1
PLA/CNs	10%	7: 1:0	dichloromethane/DMF	3:1	1
PLA/CNs	10%	11:1:0	dichloromethane/DMF	3:1	1
PLA/CNs	10%	17:1:0	dichloromethane/DMF	3:1	1
PLA/CNs/HA	10%	7:1:5	dichloromethane/DMF	3:1	1
PLA/CNs/HA	10%	11:1:5	dichloromethane/DMF	3:1	1
PLA/CNs/HA	10%	17:1:5	dichloromethane/DMF	3:1	1

After adding the dichloromethane to PLA, CNs suspension was added. HA was also added to three of the solutions. All the solutions were sonicated for one hour until complete dissolution of PLA and homogenization of solution.

2.3 Fiber mats preparation by electrospinning

All solutions were electrospun following the horizontal electrospinning set up using a grounded rotating drum as collector plate to promote fiber orientation (Figure 20).

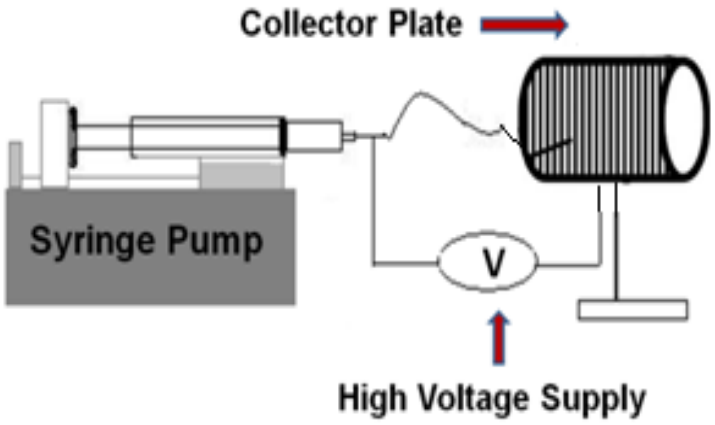

Figure 20. Horizontal electrospinning set up with rotating drum as fiber collector plate

The solutions were injected using a 10 ml disposable syringe with a 22-G needle connected to the positive terminal of the high voltage supply. The applied voltage was kept at 18kV, the distance between the tip of the needle and the collector plate was 10 cm, and the flow rate of the solution was always kept at 20µl/min, controlled by a syringe pump. The collector plate was covered with aluminum foil.

2.4 Scanning Electron Microscopy (SEM)

Morphology of the fiber mats was analyzed by using the Scanning Electron Microscopy (SEM). In this technique an electron bombardment (primary electrons) is irradiated on the surface of a specimen (Figure 21). The signals produced from the interaction of the electron beam with the sample include secondary electrons, x-rays, and other photons of different energies [83]. Secondary and backscattered electrons give information of surface topography, while x-rays emitted can give qualitative and quantitative information of the sample.

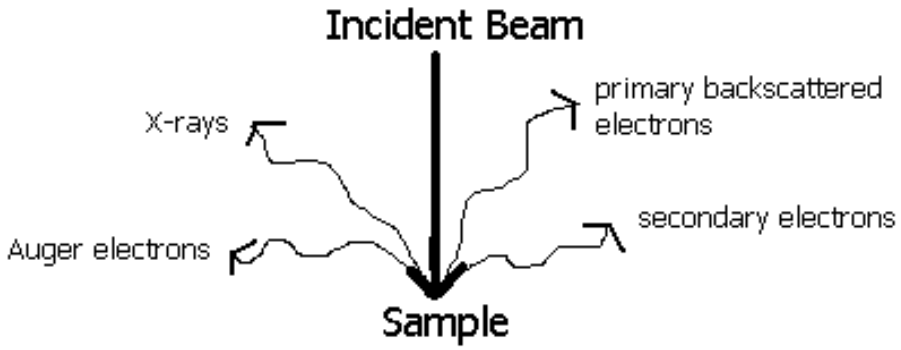

Figure 21. Electrons and x-rays ejected from the sample during electron beam bombardment [84]

The SEM can characterize organic and inorganic materials on a nanometer to micrometer scale having a magnification range of 10-10,000x. For this project a field emission scanning electron microscope (FE-SEM) with a JEOL-6400F microscope operated with an accelerating voltage of 5kV and a working distance of 20 mm was used (Figure 22).

Figure 22. Field emission scanning electron microscope (FE-SEM) JEOL-6400F

2.4-1 Sample Preparation for SEM

Non-metals need to be made conductive by covering the sample with a layer of conductive material using sputter coater [84]. The sputter coater uses an electric field and argon gas that causes an electron to be removed from the argon, making the atoms positively charged. The argon ions are attracted to a negatively charged gold foil and the gold atoms settle onto the surface the sample. In this project the samples were placed in a chamber with applied vacuum. Due to the fragile nature of PLA, in order to prevent from melting during the coating, the sample height was adjusted as shown in Figure 23. The samples were sputtered with a thin layer of gold/palladium (Au/Pd) using the following conditions: voltage: 500V, current: 10 mA, pressure: 200 mT and time: 2 min (Figure 24). Fibers diameter and diameter distribution were analyzed using 4-Pi EDS/Digital Imaging system.

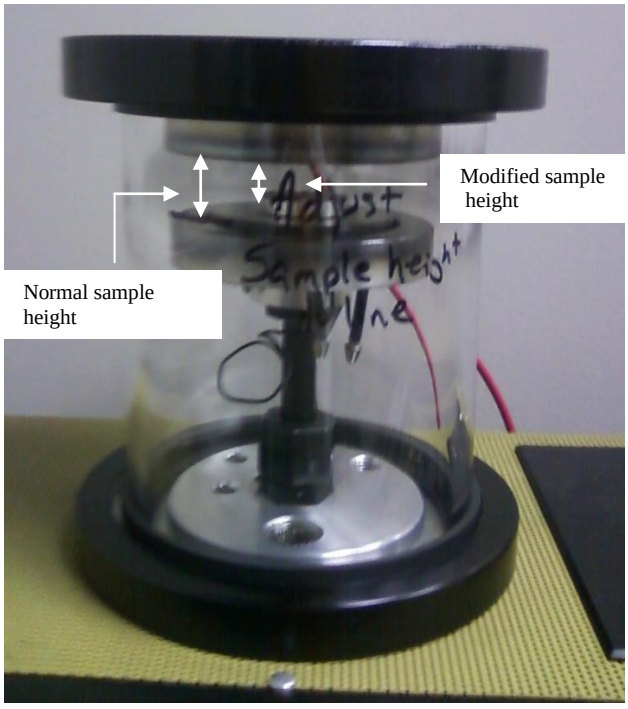

Figure 23. Chamber used for (Au/Pd) sputter coating of the samples

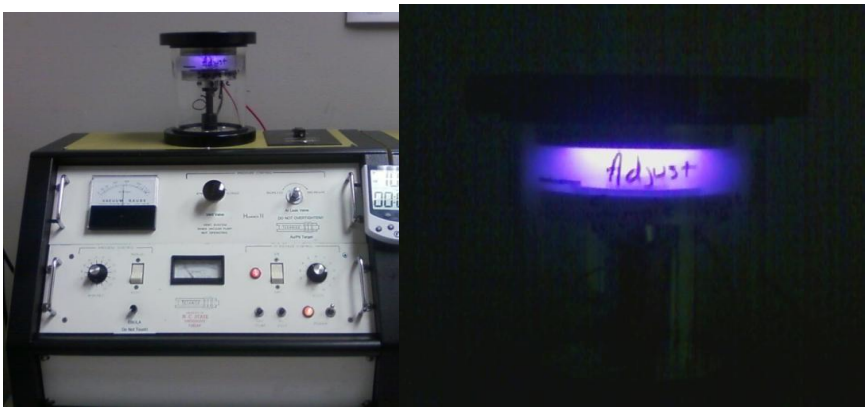

Figure 24. During sputter coating argon atoms are ionized before they reach the gold target and cause an emission of gold from the cathode to the specimen surface of the anode causing a violet light emission.

2.5 Transmission Electron Microscopy (TEM)

Transmission Electron Microscopy was used to characterize the PLA/CNs fibers. This technique uses an electron gun as the illumination source in a column that contains a series of lenses, the specimen and the imaging system [85] (Figure 25).

Figure 25. Transmission Electron Microscope [86]

This microscope, as in light microscopy, uses a condenser lens to focus the illuminating beam onto the sample and an objective lens to produce a focused and magnified image of the illuminated area (Figure 26). The projector lenses magnified the image of the specimen onto the imaging system. The specimen should be approximately 0.1 micron or less for the TEM. PLA/CNs fiber mats were observed with a Hitachi HF2000 TEM operated at an accelerating voltage of 80 kV.

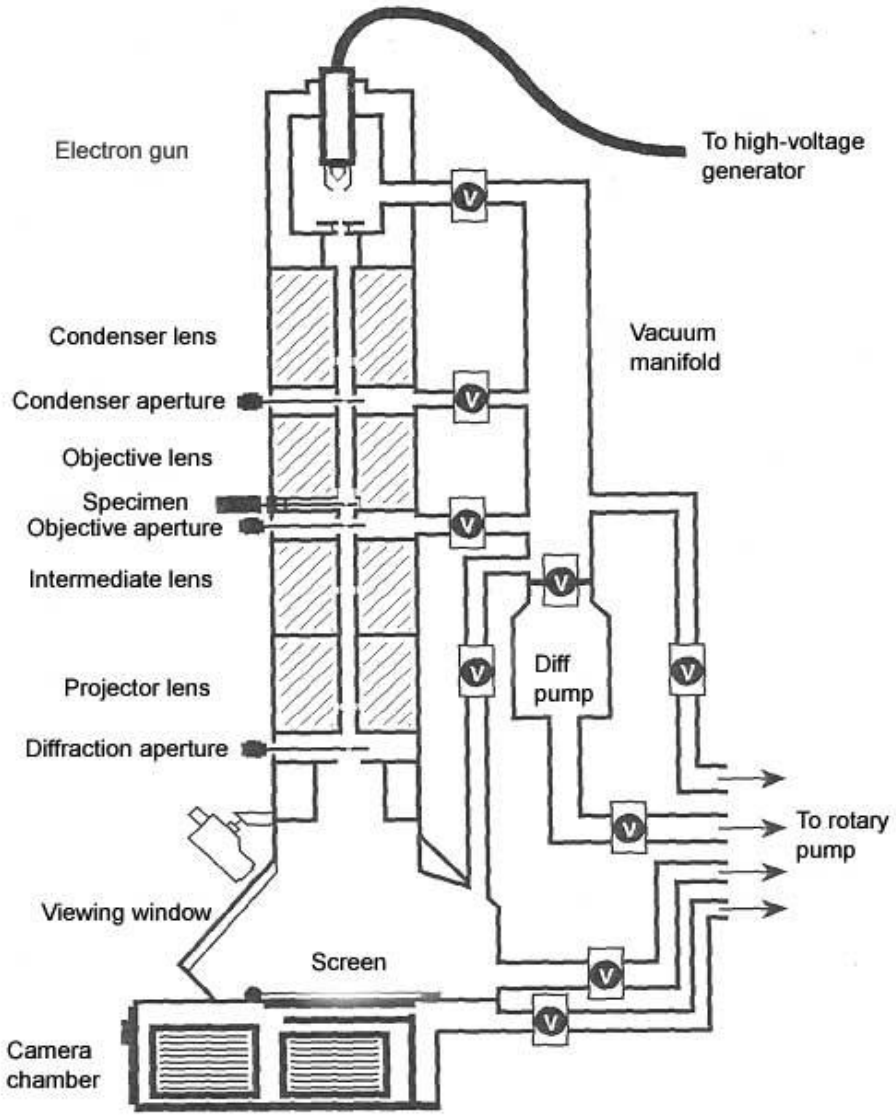

Figure 26. Schematic of a Transmission Electron Microscope column [87]

2.5-1 Sample Preparation for TEM

A blend solution of PLA/CNs was prepared and electrospun onto a carbon coated (20-30 nm thick) 400 mesh grid. The parameters used for the electrospinning are the following: voltage: 18 kV, solution flow rate: 100 µl/min, distance from the tip of the needle to the collector plate: 10 cm.

2.6 Dynamic Contact Angle (DCA) Measurement

PLA, PLA/CNs and PLA/CNs/HA fiber mats dynamic contact angle (DCA) was measured to study surface energy of the samples. By definition contact angle "is the angle, drawn through the liquid phase, between a flat solid and an air-liquid interface when a drop is placed on a surface" [89]. If the angle is less that 90, the solid is said to be hydrophilic, while if the angle is greater than 90 it is said to be hydrophobic (Figure 28).

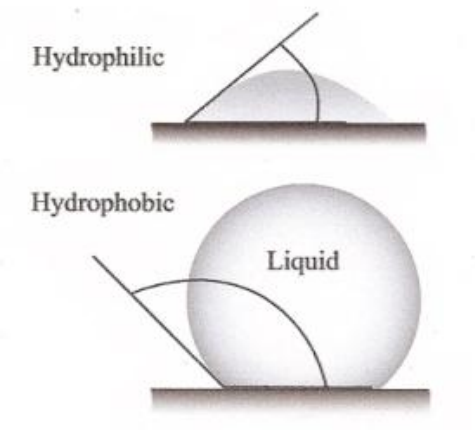

Figure 28. Contact angle in hydrophilic and hydrophobic surfaces [90]

There are different ways to measure DCA, which is the contact angle measured either when the liquid drop still spreads or its thermodynamic state conditions still change [90].

In this project the axissymmetric drop shape analysis (ADSA) technique was used (SEO Phoenix Dynamic Contact Angle) (Figure 29). For this measurement, the samples were cut and placed on the test cell. The drop was gently deposited on the sample surface by the delivering syringe. Images were taken every 30 seconds for a time range of 5 minutes. The angles were measured using Image J software.

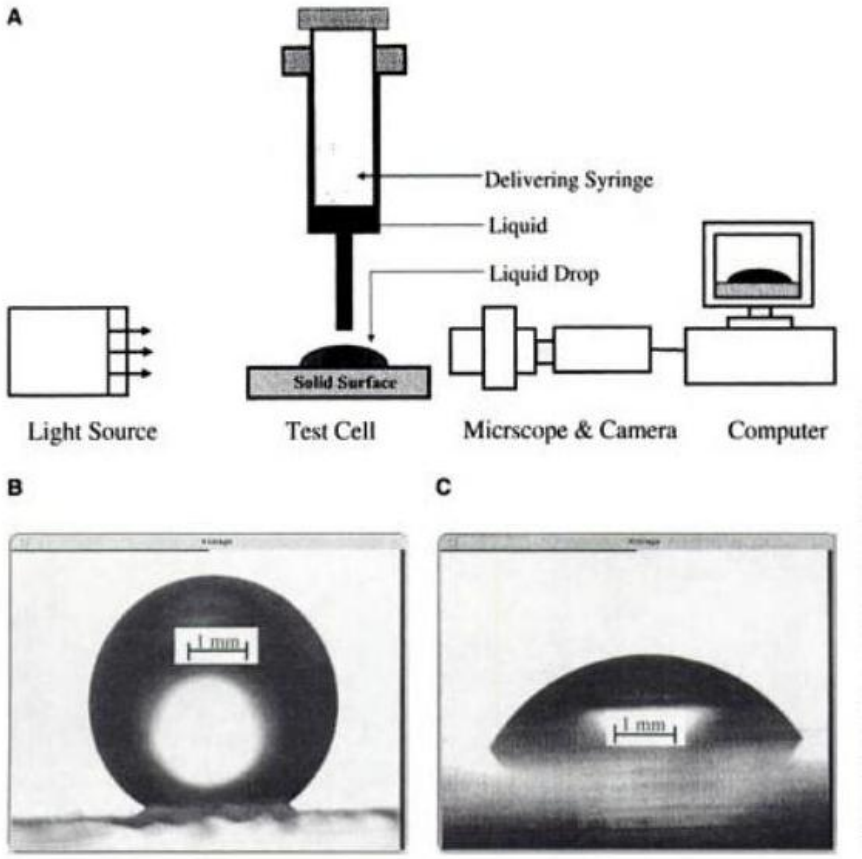

Figure 29. Axissymmetric drop shape analysis (ADSA) set up [91]

2.7 Dynamic Mechanical Analysis (DMA)

Dynamic Mechanical Analysis (DMA) was performed to measure out the tensile strength of PLA, PLA/CNs, and PLA/CNs/HA fiber matrices. DMA can be described as applying

an oscillating force to a sample and analyzing the material's response to that force [92]. By doing this we are able to measure the stiffness and damping, which are reported as modulus and tan delta. The applied force is called stress and the deformation that results from this force is called strain. The slope of the line gives the relationship of stress to strain and is measure of the modulus which is dependent on the temperature and the applied stress. For this project the TA Instrument Q800 in tensile mode was used (Figure 30). The samples were cut in approximately 1 in^2 to be analyzed. DMA test was kept isothermal at a temperature of 25^oC. Ramp force used was from 3.0 N/min up to 18 N.

Figure 30. Dynamic Mechanical Analysis Equipment [93]

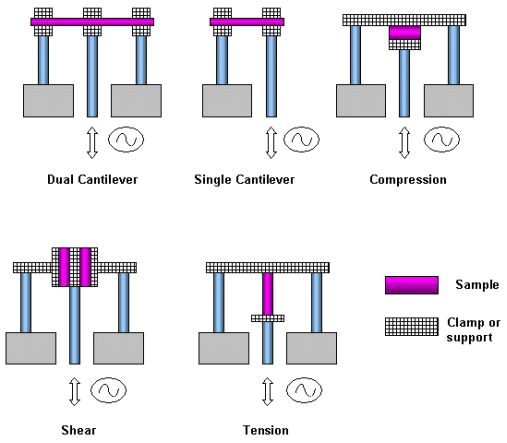

Figure 31. A typical instrument for performing DMA can deform the sample in a number of different ways as illustrated above [94]

2.8 Thermogravimetric Analysis (TGA)

Thermogravimetric Analysis was performed to corroborate the presence of CNs in the PLA fiber matrix. In this technique the mass of a polymer is measured as a function of temperature or time while the sample is subjected to a controlled temperature program in a controlled atmosphere [95]. During the process polymers usually exhibit mass loss, which can give useful information of the material such as composition, extent of cure, and thermal stability. The general instrument set up is shown in Figure 32.

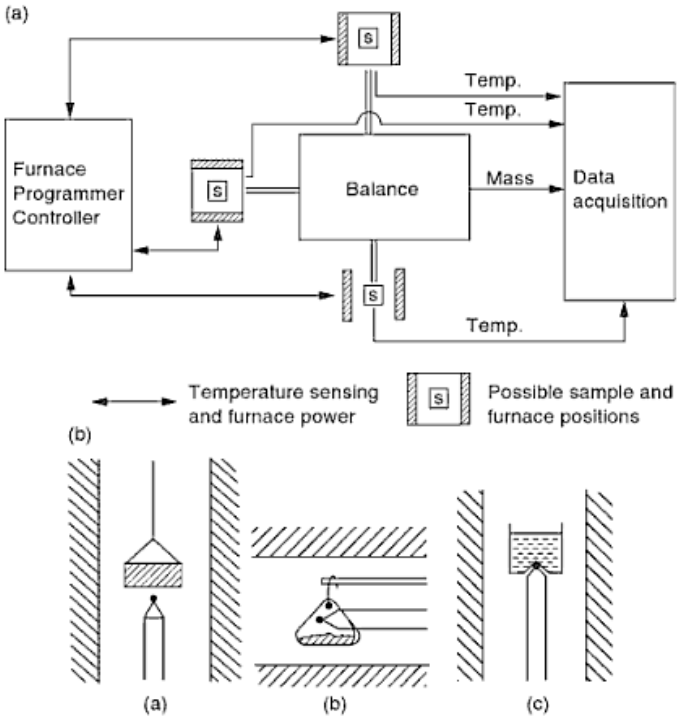

Figure 32. (a) General arrangement of the components in a thermobalance; (b) typical location of thermocouples [95]

For this project, a TA Instruments Q500 Thermogravimetric Analyzer was used. Electrospun PLA fibers mats were cut, weighed out and placed on a platinum pan. Samples were analyzed using the following procedure: Starting at a temperature of 30^{o}C, the temperature was increased 20^{o}C/min up to 600^{o}C; nitrogen flow was kept at 40

ml/min-60 ml/min. Degradation temperature peaks were analyzed in order to have information of the composition of the material.

2.9 Differential Scanning Calorimetry (DSC)

Differential Scanning Calorimetry (DSC) was performed to study the crystallinity of the PLA, PLA/CNs and PLA/CNs/HA electrospun fibers. DSC is the measurement of the change of the difference in the heat flow rate to the sample and to a reference sample while they are subjected to a controlled temperature program [96]. This technique allows the heat flow rates and their changes at specific temperatures, to be quickly measured on small sample masses, in wide temperature ranges and with accuracy. It is usually applied in many fields for materials characterization, comparison measurements, stability investigations, evaluation of phase diagrams, determination of heat capacity, etc. Figure 33 shows the general instrument set up.

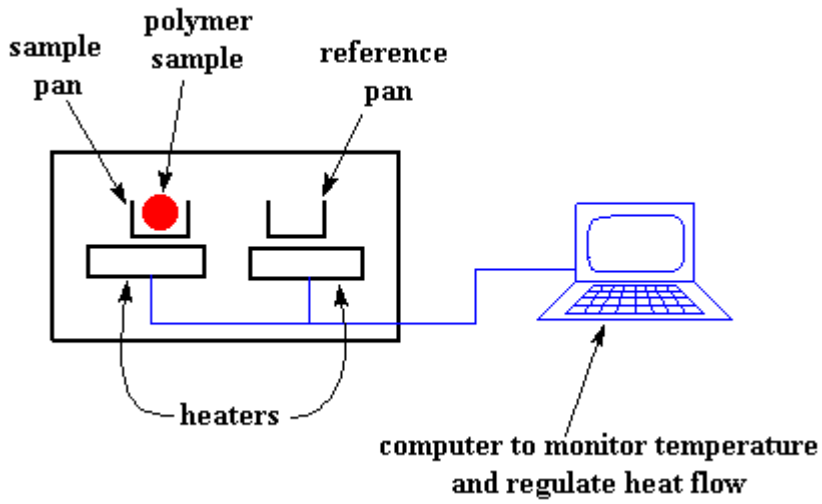

Figure 33. Typical Differential Scanning Calorimeter Schematic [97]

In this project DSC was performed using a TA Instruments Q100 differential scanning calorimeter. In a typical experiment 10 mg of sample were placed on an aluminum pan

and heated from -80^{o}C to 200^{o}C at a rate of 10^{o}C/min. Nitrogen flow was kept at 50 ml/min. The melting temperature (T_m) was taken as the onset temperature of the melting endotherms of the sample. Crystallinity was calculated using a formula that will be presented at the results and discussion section.

2.10 Cell culture

In order to study the cytocompatibility of the three different scaffolds prepared, cell culture was performed using human adipose derived mesenchymal stem cells (AD-MSCs). Scaffolds were soaked in 70% ethanol for 15 minutes as a sterilization procedure. They were washed with PBS twice for about 5 minutes and then soaked in complete growth medium for two days. They were seeded with 100,000 cells on each scaffold and grew in complete growth medium for one week. Life/dead assay and confocal microscopy were performed in order to study cell viability. This fluorescence based assay allows the examination of animal cells, bacteria and fungi. Fluorescent dyes used in the viability test range from blue to near-IR emission. In confocal microscopy the dye in the specimen is excited by the laser light and fluoresces [98]. The fluorescent green light is descanned by mirrors that scan the excitation light (blue) from the laser and then passes through the dichroic mirror. Then, it is focused onto the pinhole. The light that makes it through the pinhole is measured by a detector such as a photomultiplier tube. The detector is attached to a computer, which builds up the image one pixel at a time. Figure 34 shows the basic set up of a confocal microscope.

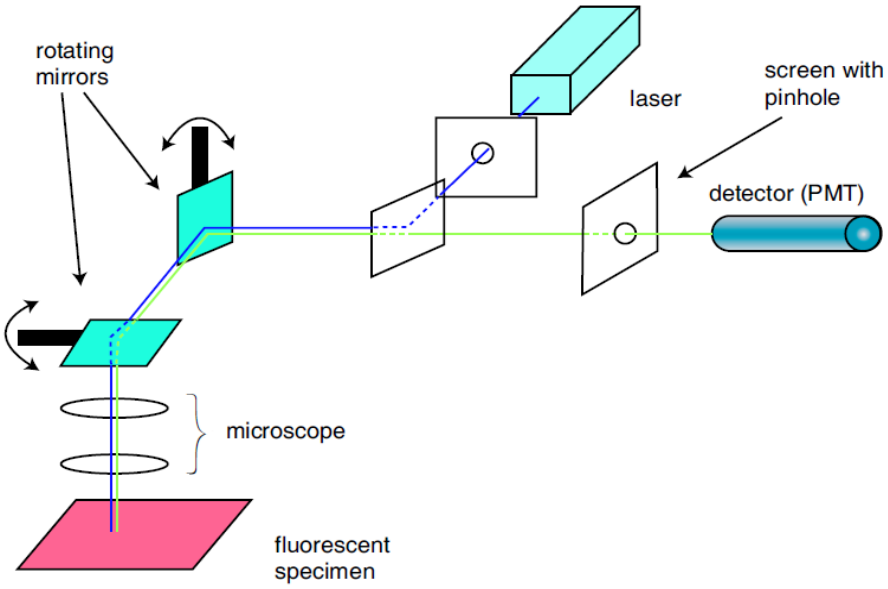

Figure 34. Basic setup of a confocal microscope. Light from the laser is scanned across the specimen by the scanning mirrors. Optical sectioning occurs as the light passes through a pinhole on its way to the detector [98]

Chapter 3

Results and Discussion

3.1 Morphology Characterization by SEM

PLA, PLA/CNs and PLA/CNs/HA electrospun fiber mats were obtained as shown in

Figure 35.

Figure 35. PLA fiber mat representative of all samples prepared

Fiber mat morphology was analyzed using SEM. Randomly oriented fiber mats were obtained for all three nanocomposites instead of aligned fiber mats (Figure 36-42).

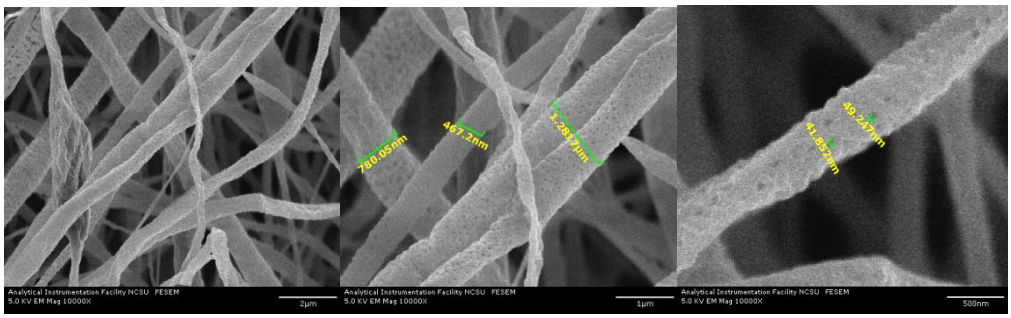

Figure 36. Pure PLA Electrospun Fibers

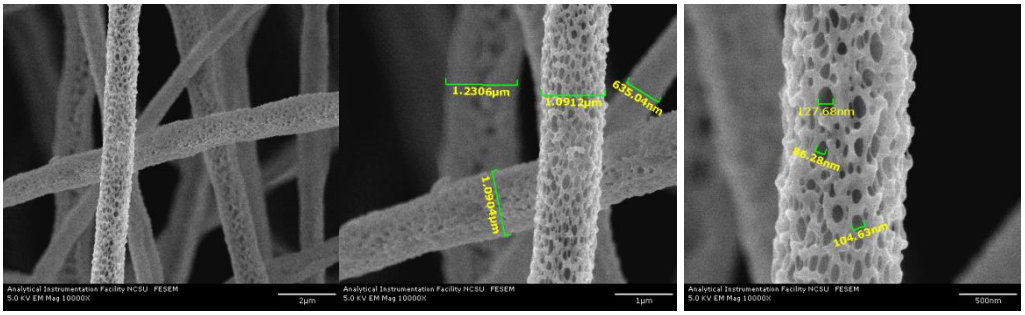

Figure 37. PLA/CNs Electrospun Fibers from 7:1 ratio solution

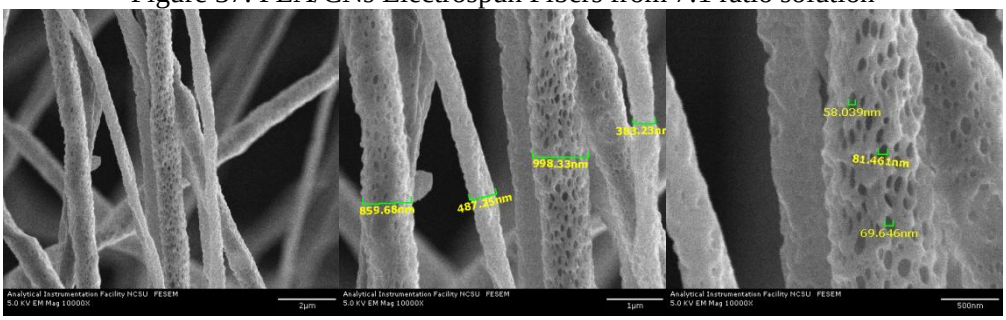

Figure 38. PLA/CNs Electrospun Fibers from 11:1 ratio solution

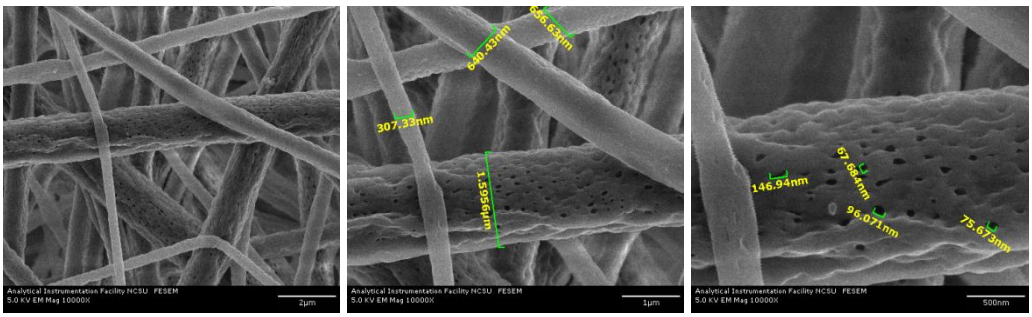

Figure 39. PLA/CNs Electrospun Fibers from 17:1 ratio solution

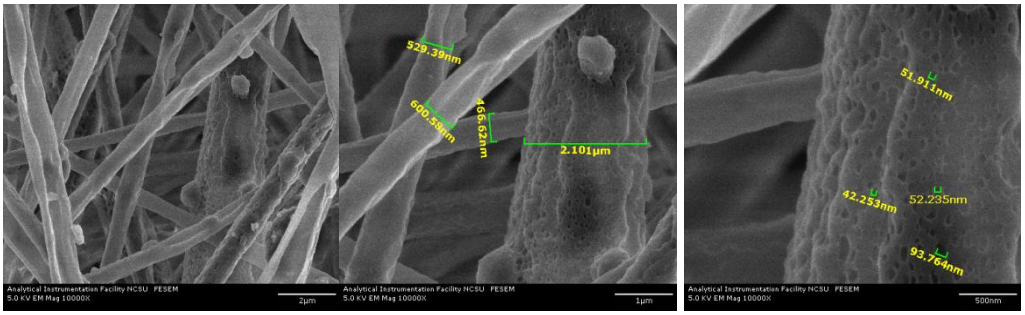

Figure 40. PLA/CNs/HA Electrospun Fibers from 7:1:5 ratio solution

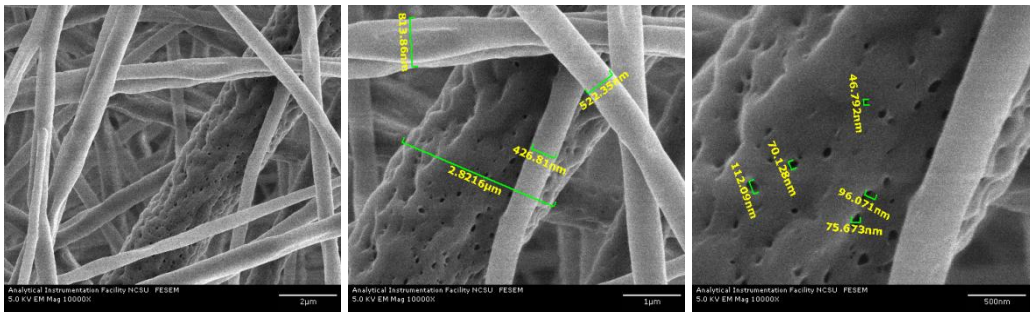

Figure 41. PLA/CNs/HA Electrospun Fibers from 11:1:5 ratio solution

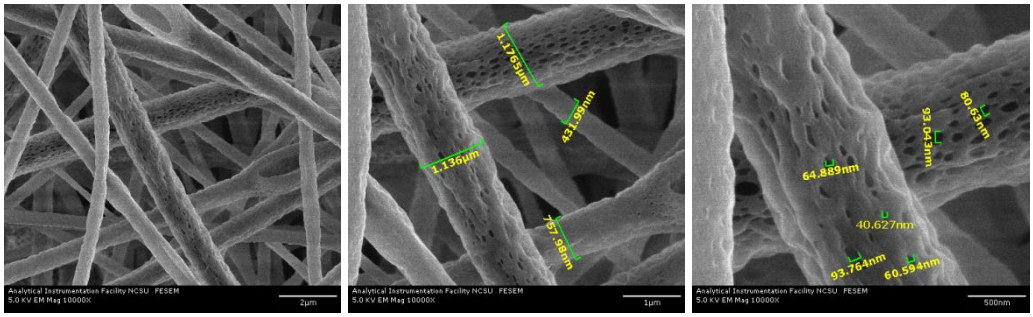

Figure 42. PLA/CNs/HA Electrospun Fibers from 17:1:5 ratio solution

It was expected to obtain aligned fibers with the use of the rotating drum collector plate. However, randomly oriented were obtained, probably due to a slow rate of rotation. Fibers diameters for all the nanocomposites ranged between 300 nm-2000 nm (2µm) in size. Surprisingly, very well defined pores were obtained along the fibers for all the nanocomposites. However, the PLA/CNs 7:1 nanocomposite shows bigger and more evenly dispersed pores along the fibers. It is believed that during the process of electrospinning, the dichloromethane was being evaporated while the DMF having a

higher boiling point (153^{o}C) stayed in the fiber and evaporated over time allowing the formation of pores. The reason that pore amount in the PLA/CNs 7:1 nanocomposite were higher can be understood as a higher interaction of DMF with the CNs. DMF is a highly polar aprotic (no H^{+} can be donated) solvent with a dipole moment of 3.82. DMF and CNs stable interaction takes place due to the strong dipole moment of DMF and the negatively charge surfaces of CNs due to the sulfate groups that remained from acid hydrolysis. Since the fiber mat in Figure 37 has the highest content of CNs, it will have higher interactions with DMF and result in very well defined highest pore amount. It is very clear from all the images that the pore distribution decreases as the CNs content was decreased. Figure 40 with the highest CNs content (from all three PLA/CNs/HA nanocomposites) clearly shows the deposition of HA on the surfaces of the fiber. For the fibers with lower content of CNs, HA cannot be seen as deposited on the surface and can probably be incorporated inside the fiber due to the low content of CNs and no competition taking place.

3.2 Electrospun Fiber Mats Characterization by TEM

Cellulose Nanocrystals incorporation was analyzed by TEM. PLA/CNs fiber mats from the 7:1 ratio solution were prepared for this analysis.

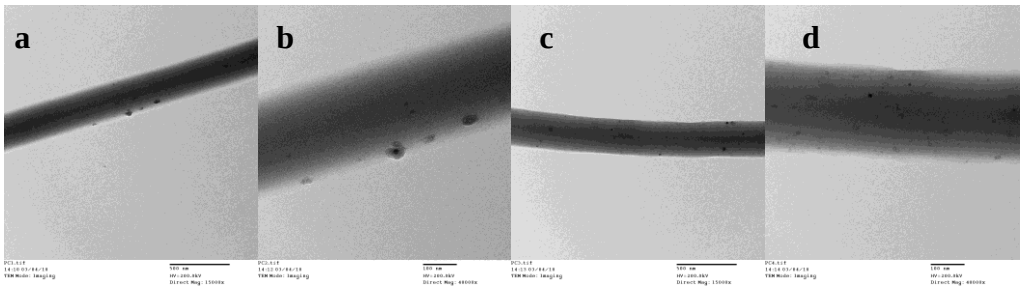

Figure 43. Cellulose Nanocrystals incorporated intoPLA fibers (from PLA/CNs 7:1 solution)

Figure 43-c,d shows an even dispersion of CNs along the PLA fiber matrix. For some fibers (Figure 43-a, b) it is clearly seen the aggregation of CNs due to the strong hydrogen bond interactions between the nanocrystals.

3.3 Surface Energy Study by Contact Angle Measurement

Dynamic contact angle measurement was performed by taking consecutive images of a drop of water on the surface of the sample for a time frame of 5 minutes.

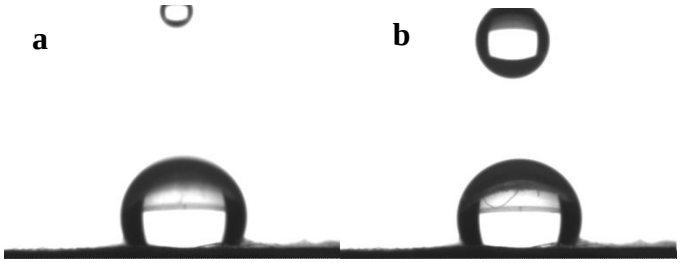

Figure 44. Pure PLA fiber matrix dynamic contact angle measurement (a) initial contact angle at 0 min (b) contact angle at 5 mins

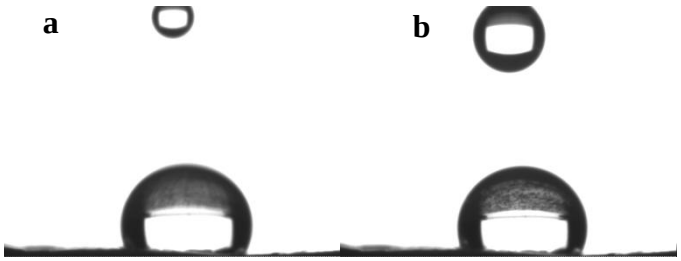

Figure 45. PLA/CNs (7:1) fiber matrix dynamic contact angle measurement (a) initial contact angle at 0 min (b) contact angle at 5 mins

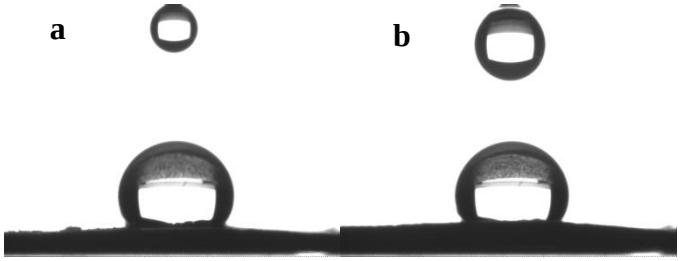

Figure 46. PLA/CNs (11:1) fiber matrix dynamic contact angle measurement (a) initial contact angle at 0 min (b) contact angle at 5 mins

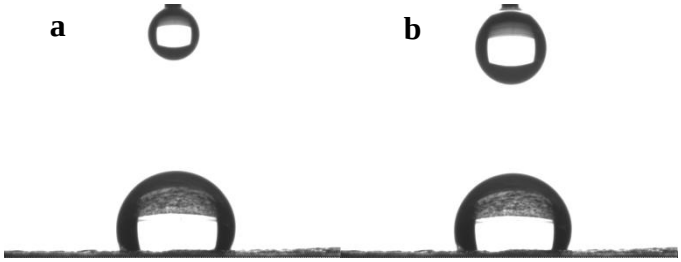

Figure 47. PLA/CNs (17:1) fiber matrix dynamic contact angle measurement (a) initial contact angle at 0 min (b) contact angle at 5 mins

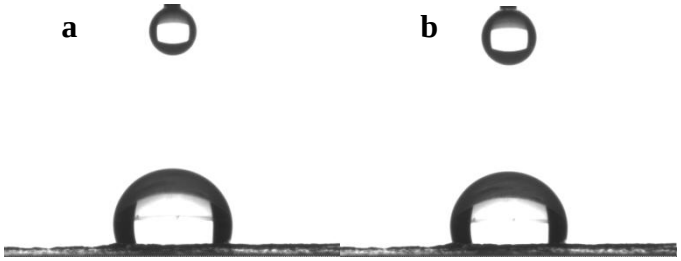

Figure 48. PLA/CNs/HA (7:1:5) fiber matrix dynamic contact angle measurement (a) initial contact angle at 0 min (b) contact angle at 5 mins

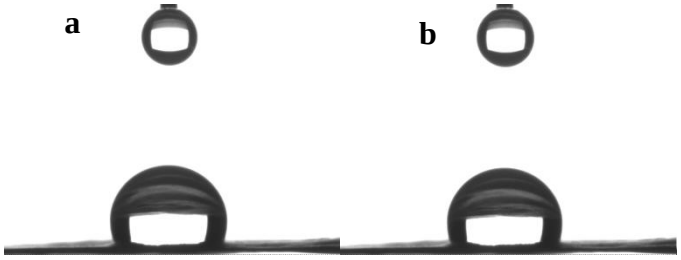

Figure 49. PLA/CNs/HA (11:1:5) fiber matrix dynamic contact angle measurement (a) initial contact angle at 0 min (b) contact angle at 5 mins

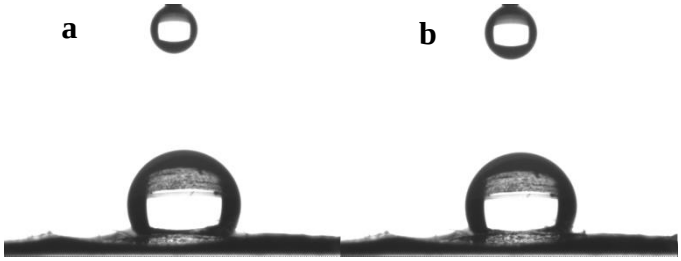

Figure 50. PLA/CNs/HA (17:1:5) fiber matrix dynamic contact angle measurement (a) initial contact angle at 0 min (b) contact angle at 5 mins

From Figures 44 to 50 it is clearly seen that the contact angle for all the nanocomposites was more than 90^{o} which means that all of them are hydrophobic. The contact angles were measured using Image J software and further analyzed using Microsoft Excell. As seen in Figure 51 initial contact angles were higher for the PC-11 than for any other nanocomposite. It was expected to find higher contact angles for pure PLA than for any other nanocomposite since this is a hydrophobic polymer matrix. However, the roughness of the sample can also be a limiting factor for water penetration, and this could be the case for PC-11. We can also see that initial contact angle for the nanocomposites that contain HA nanoparticles are lower due to the hydrophilic nature of hydroxyapatite.

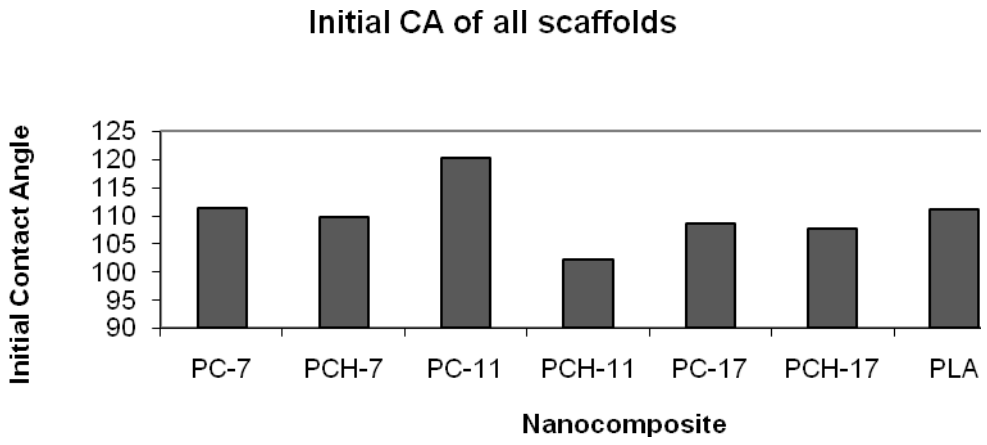

Figure 51. Initial contact angle (0 min) of all nanocomposites scaffolds; PLA (Pure PLA), PC-7 (PLA/CNs 7:1), PCH-7 (PLA/CNs/HA 7:1:5), PC-11 (PLA/CNs 11:1), PCH-11 (PLA/CNs/HA 11:1:5), PC-17 (PLA/CNs 17:1), PCH-17 (PLA/CNs/HA 17:1:5)

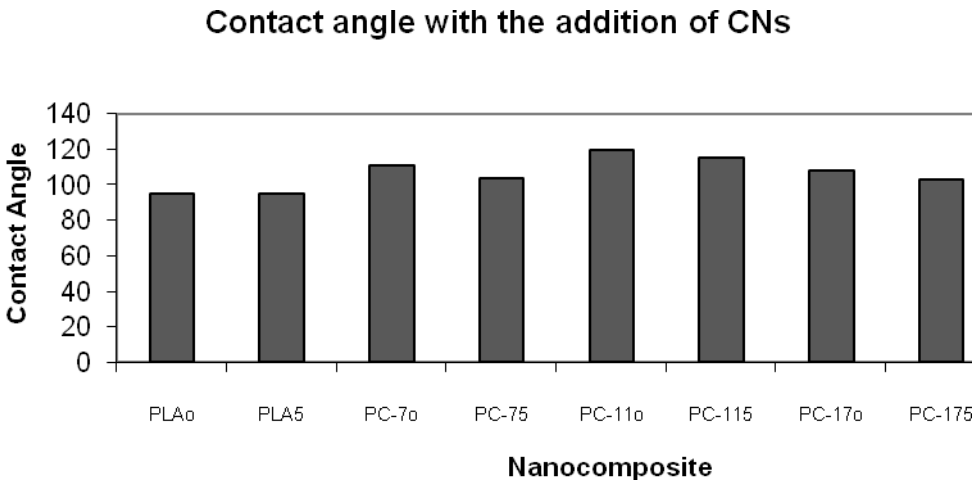

Figure 52. Dynamic Contact Angle (0-5 min) of nanocomposites scaffolds; PLA (Pure PLA), PC-7 (PLA/CNs 7:1), PC-11 (PLA/CNs 11:1), PC-17 (PLA/CNs 17:1), For all of them (o) means 0 min; (5) means 5 mins

As seen in Figure 52, contact angles for all the CNs nanocomposites slightly decreased over time due to the addition of CNs to the PLA matrix. However PLA contact angle remained the same over time.

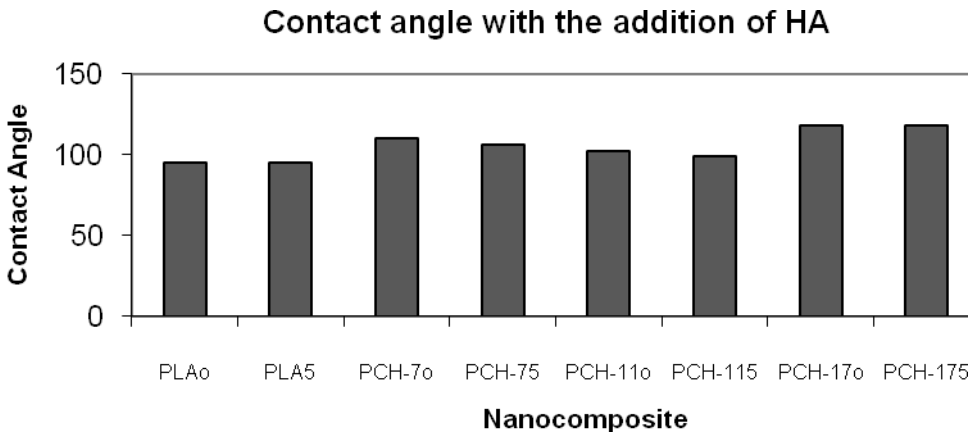

Figure 53. Dynamic Contact Angle (0-5 min) of nanocomposites scaffolds; PLA (Pure PLA), PCH-7 (PLA/CNs/HA 7:1:5), PCH-11 (PLA/CNs/HA 11:1:5), PCH-17 (PLA/CNs/HA 17:1:5). For all of them (o) means 0 min; (5) means 5 mins

For all the nanocomposites that contain HA nanoparticles the contact angle slightly decreased over time (Figure 53). Pure PLA contact angles remained the same over time.

3.4 Mechanical Properties by Dynamic Mechanical Analysis

DMA was performed to measure out the tensile strength of the nanocomposite scaffolds. Figures 54 to 60 show the stress and strain diagram for pure PLA and the nanocomposites. Table 8 shows the tensile strength values for pure PLA and the nanocomposite scaffolds. As expected, the lowest tensile strength value was obtained for pure PLA. However a different trend to what it was expected was found for the rest of the nanocomposites. The highest tensile strength was expected for the nanocomposites with highest content of CNs. However the highest tensile strengths were obtained for the PLA/CNs (11:1) and PLA/CNs/HA (11:1:5) nanocomposites. It is hypothesized that at higher content of CNs an agglomeration is happening which decreases strength of the materials. The highest tensile strength was obtained for the nanocomposite PLA/CNs/HA (11:1:5). HA has been found to reinforce PLA fiber mats in previous work [23].

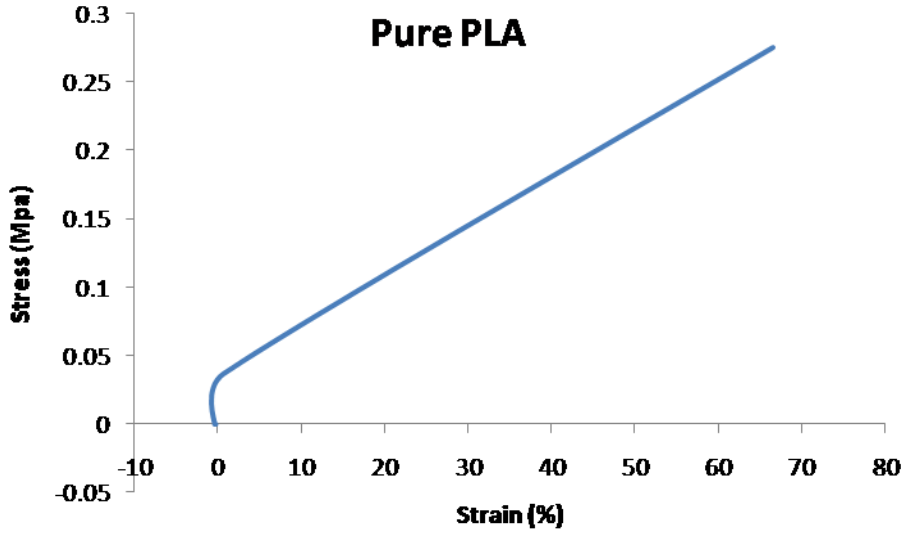

Figure 54. Stress and Strain Diagram for Pure PLA

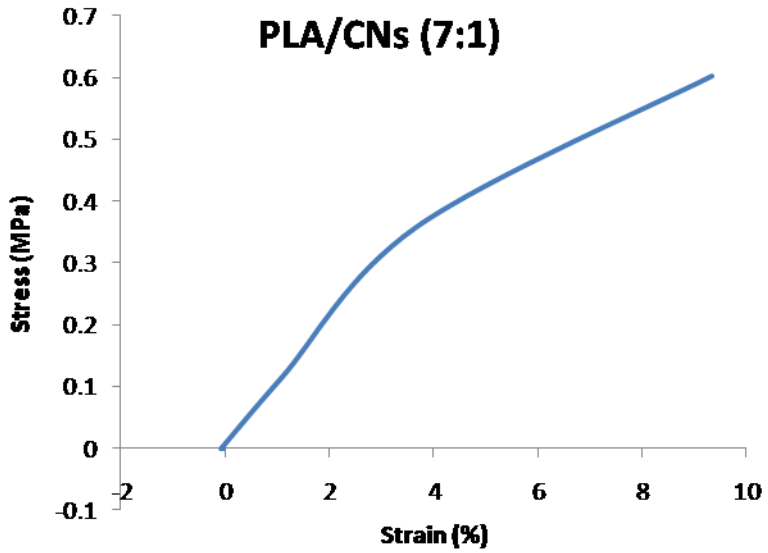

Figure 55. Stress and Strain Diagram for PLA/CNs (7:1) Nanocomposite

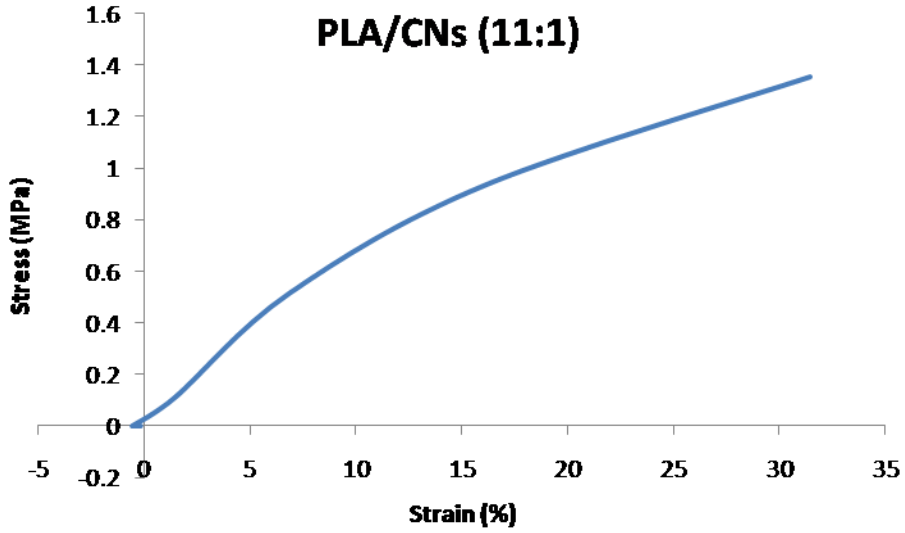

Figure 56. Stress and Strain Diagram for PLA/CNs (11:1) Nanocomposite

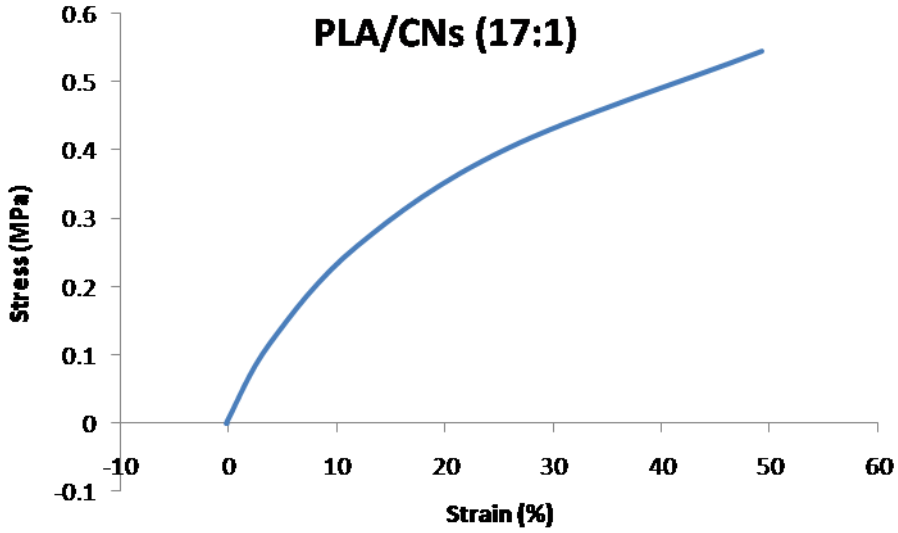

Figure 57. Stress and Strain Diagram for PLA/CNs (17:1) Nanocomposite

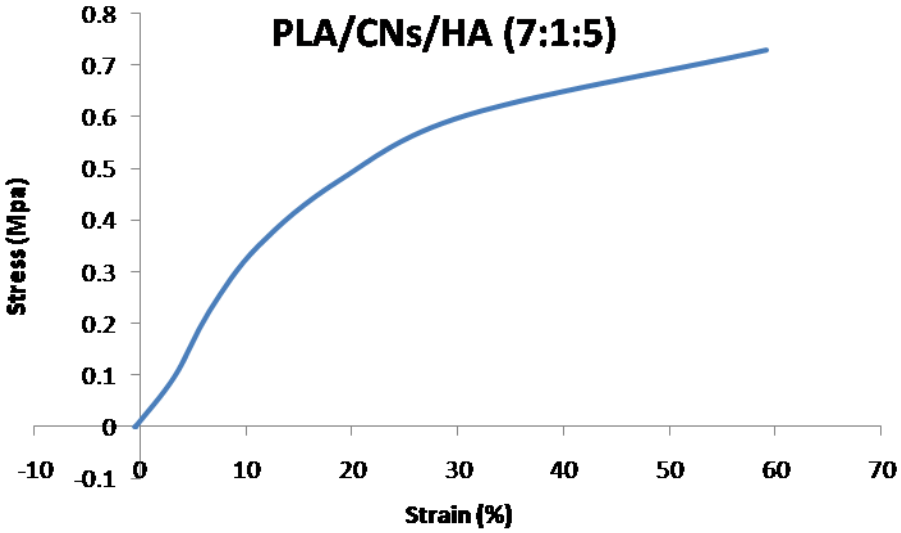

Figure 58. Stress and Strain Diagram for PLA/CNs/HA (7:1:5) Nanocomposite

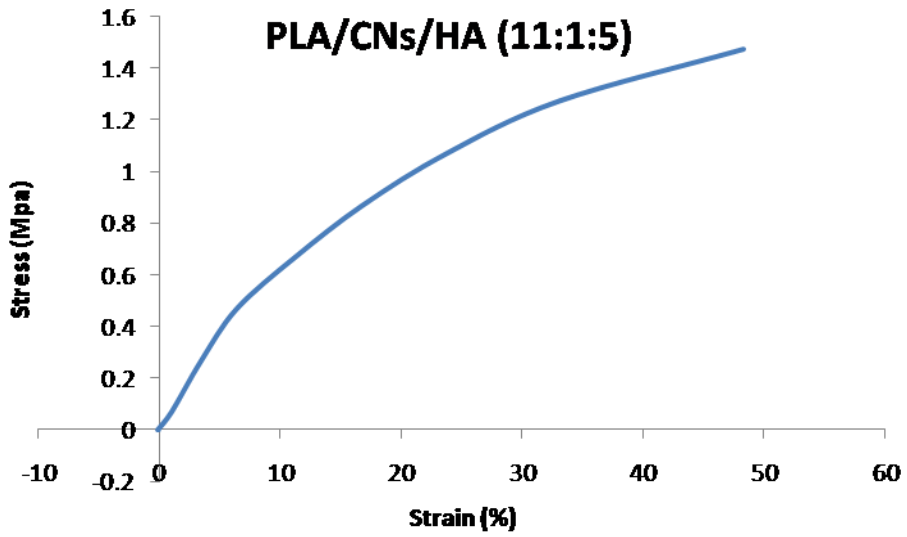

Figure 59. Stress and Strain Diagram for PLA/CNs/HA (11:1:5) Nanocomposite

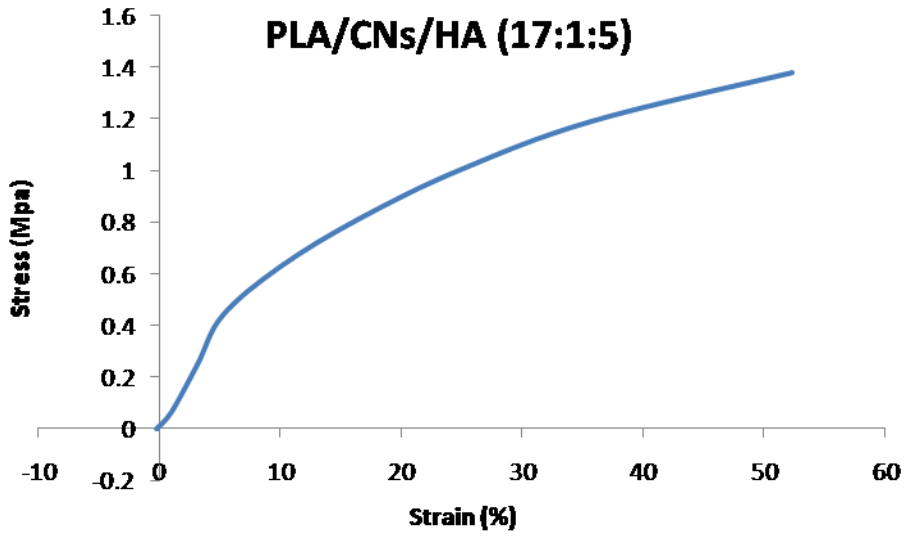

Figure 60. Stress and Strain Diagram for PLA/CNs/HA (17:1:5) Nanocomposite

Table 8. Tensile strength values obtained for all the nanocomposite scaffolds

Sample	PLA/CNs/HA ratio	Tensile strength (Mpa)
PLA	Pure	0.273
PLA/CNs	7:1	0.691
PLA/CNs	11:1	0.715
PLA/CNs	17:1	0.543
PLA/CNs/HA	7:1:5	0.759
PLA/CNs/HA	11:1:5	1.471
PLA/CNs/HA	17:1:5	1.379

3.5 Thermogravimetric Analysis

TGA was performed to confirm the presence of CNs in the fiber matrix. Degradation peak around 277^{o}C can be seen for PLA/CNs nanocomposite (7:1). For lower CNs content matrices, no CNs peak was observed. PLA peak was clearly seen around 378^{o}C (Figures 61 to 67).

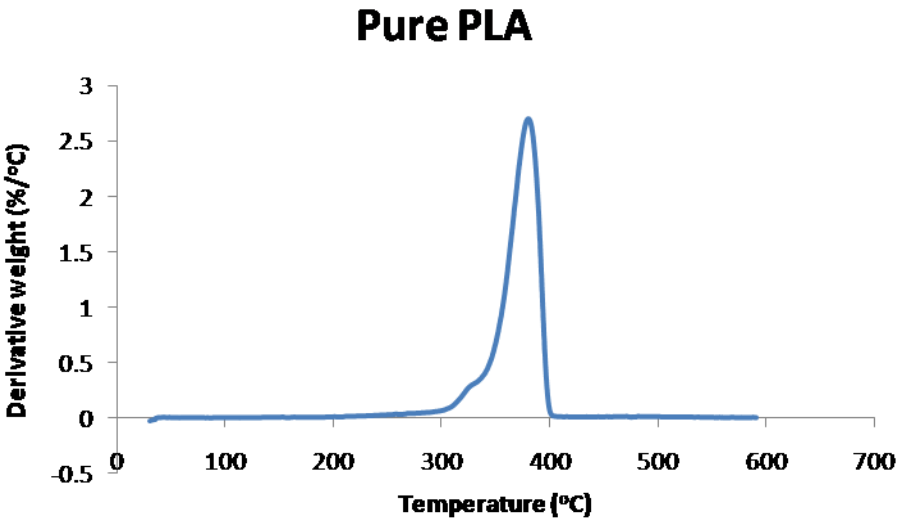

Figure 61. Derivative weight vs. temperature graph for pure PLA

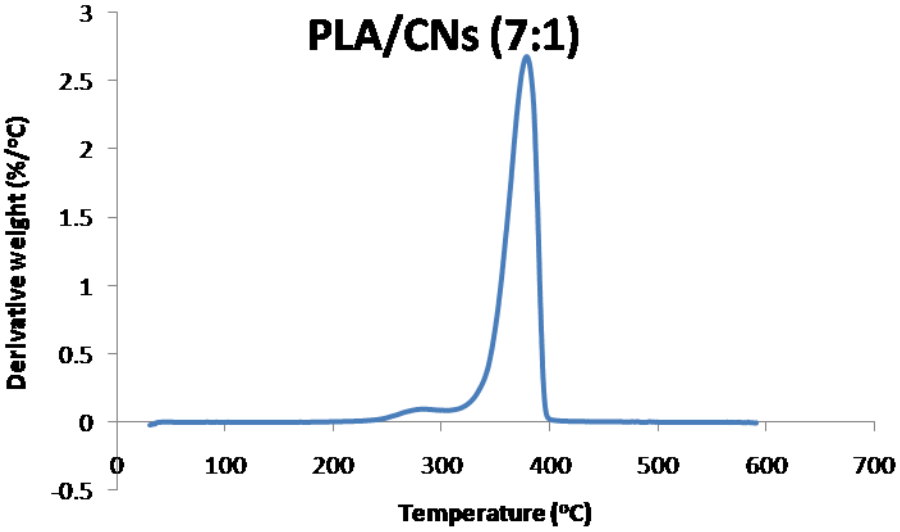

Figure 62. Derivative weight vs. temperature graph for PLA/ CNs (7:1)

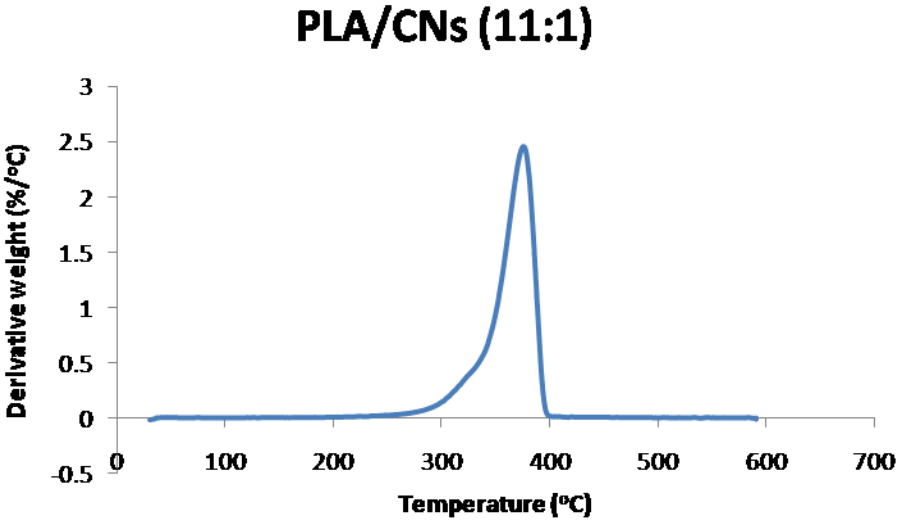

Figure 63. Derivative weight vs. temperature graph for PLA/ CNs (11:1)

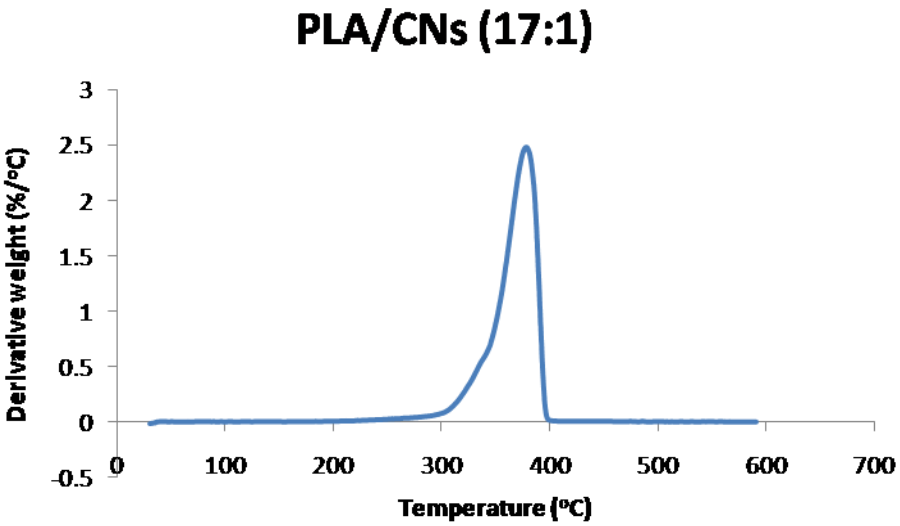

Figure 64. Derivative weight vs. temperature graph for PLA/ CNs (17:1)

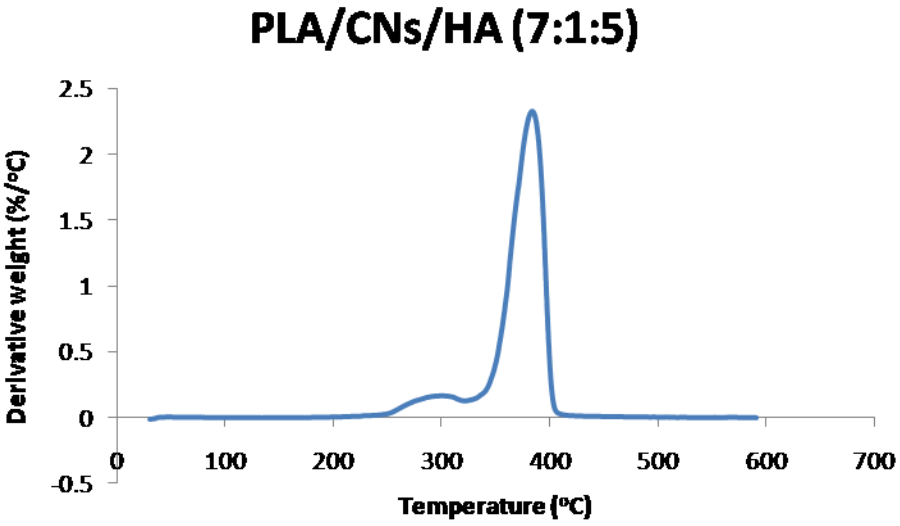

Figure 65. Derivative weight vs. temperature graph for PLA/ CNs/HA (7:1:5)

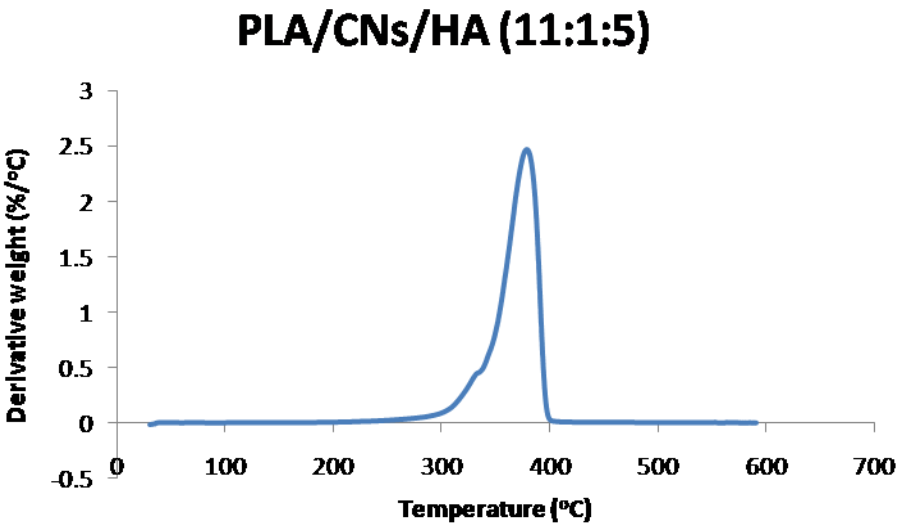

Figure 66. Derivative weight vs. temperature graph for PLA/ CNs /HA (11:1:5)

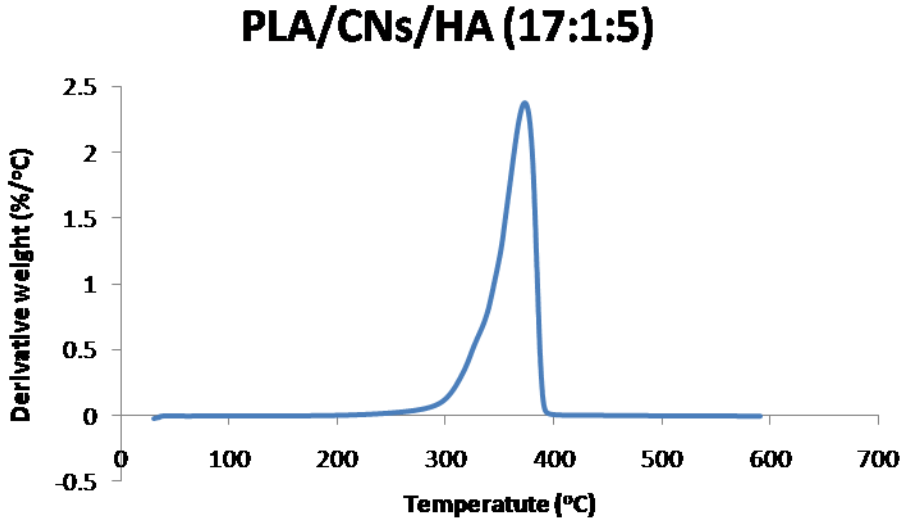

Figure 67. Derivative weight vs. temperature graph for PLA/ CNs /HA (17:1:5)

3.6 Differential Scanning Calorimetry

DSC was performed to study the crystallinity of the nanocomposites (Figures 68 to 74).

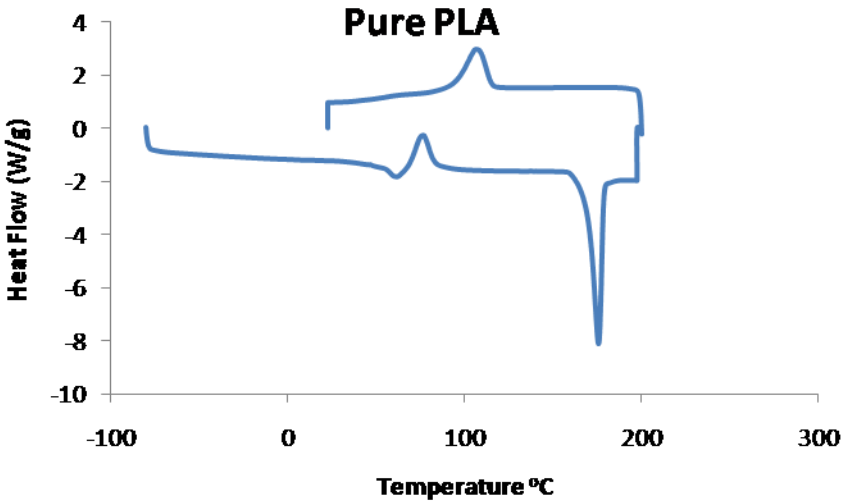

Figure 68. Heat Flow vs. Temperature plot for Pure PLA

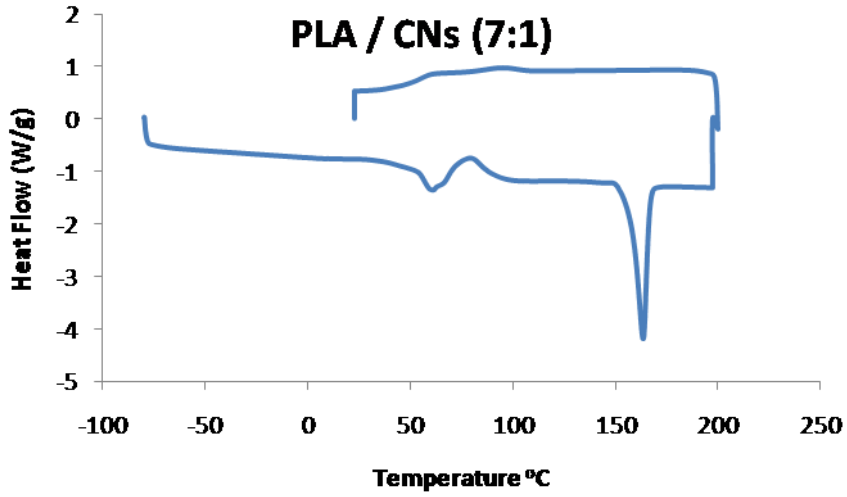

Figure 69. Heat Flow vs. Temperature plot for PLA/CNs (7:1) Nanocomposite

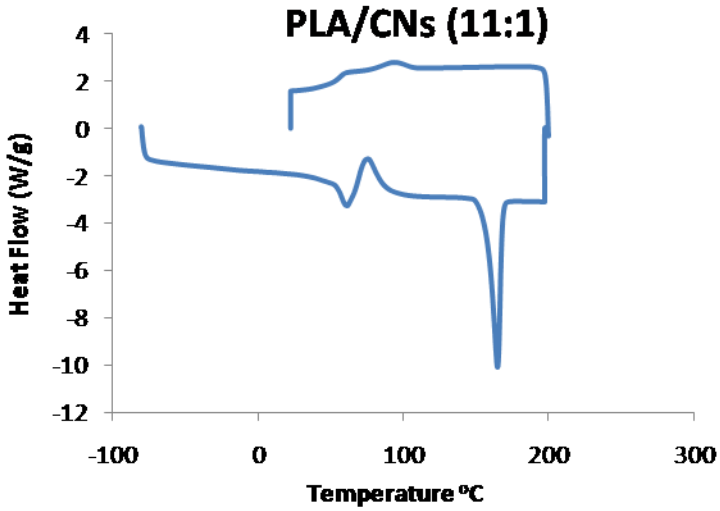

Figure 70. Heat Flow vs. Temperature plot for PLA/CNs (11:1) Nanocomposite

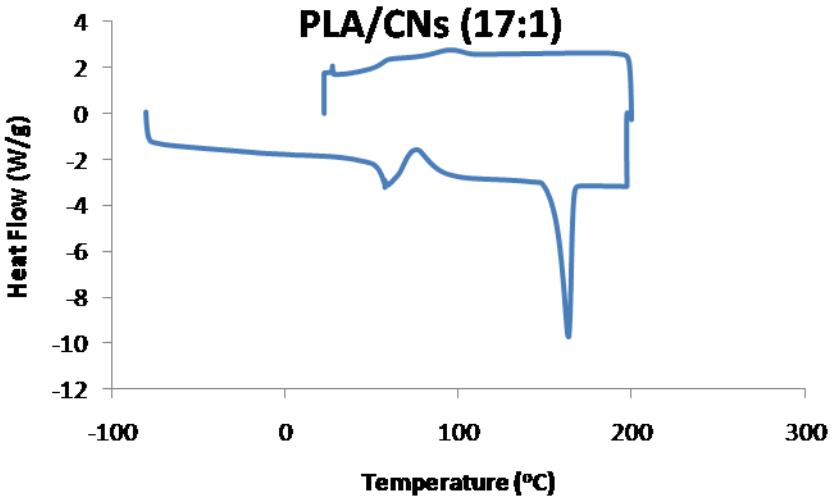

Figure 71. Heat Flow vs. Temperature plot for PLA/CNs (17:1) Nanocomposite

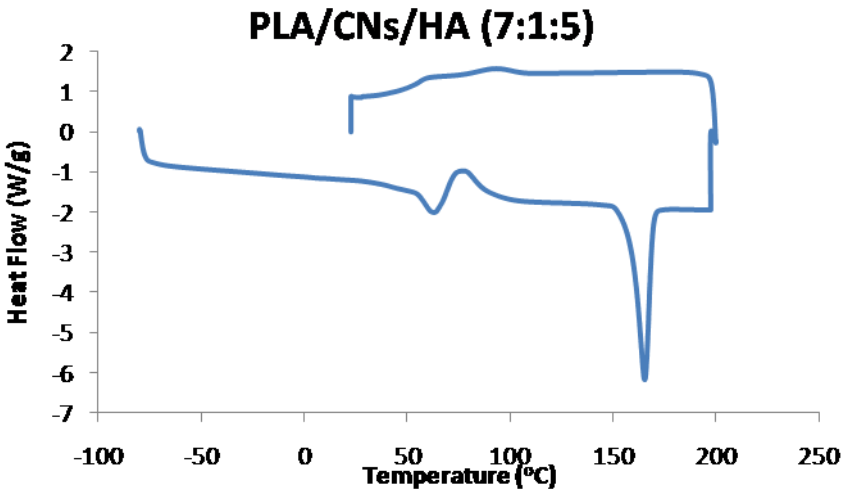

Figure 72. Heat Flow vs. Temperature plot for PLA/CNs/HA (7:1:5) Nanocomposite

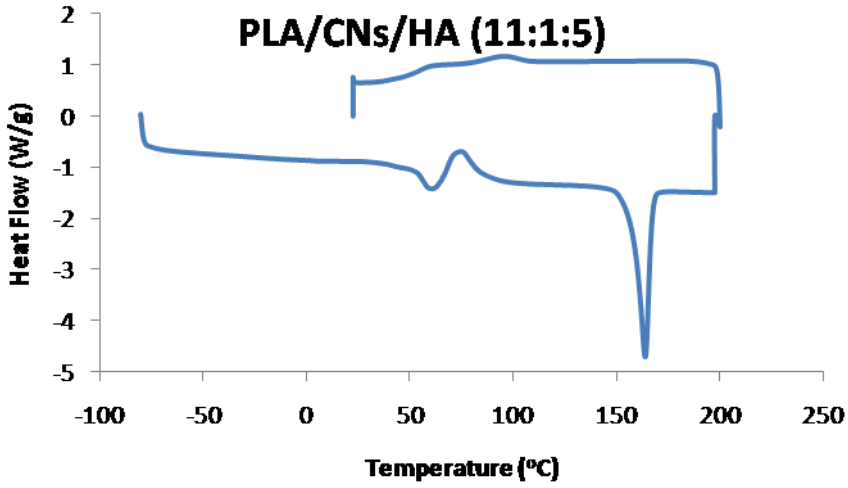

Figure 73. Heat Flow vs. Temperature plot for PLA/CNs/HA (11:1:5) Nanocomposite

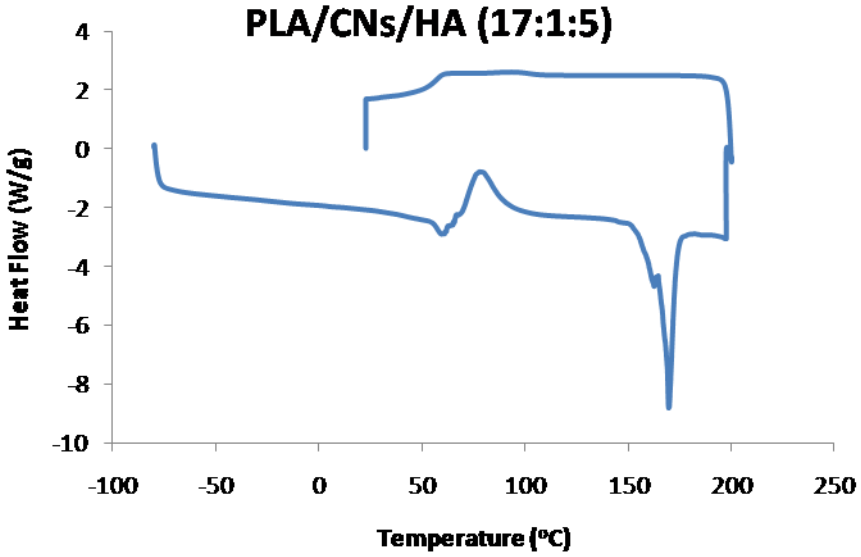

Figure 74. Heat Flow vs. Temperature plot for PLA/CNs/HA (17:1:5) Nanocomposite

Table 9. Enthalpy values obtained from DSC and calculated crystallinity

Sample	PLA/CNs/HA ratio	ΔH sample (J/g)	Crystallinity (X_c)
PLA	100%	37.77	40.6
PLA/CNs	7:1	35.47	44.3
PLA/CNs	11:1	33.43	39.4
PLA/CNs	17:1	38.24	43.4
PLA/CNs/HA	7:1:5	31.81	42.2
PLA/CNs/HA	11:1:5	40.16	50.1
PLA/CNs/HA	17:1:5	25.55	30.8

Crystallinity was calculated using the following equation:

$$\%\ of\ crystallinity = \frac{\Delta H_m\ sample}{\Delta H_m 100\%\ crystalline\ polymer} x \frac{100}{w}$$

The ΔH of 100% pure crystalline PLA is 93 J/g. As seen in Table 9 there is no correlation in the crystallinity values obtained for the nanocomposites. The highest crystallinity was obtained for the PLA/CNs/HA (11:1:5) nanocomposite while the lowest

crystallinity was obtained for PLA/CNs/HA (17:1:5) nanocomposite. It was expected to have highest crystallinity in the nanocomposites with higher content of CNs (PLA/CNs 7:1; PLA/CNs/HA 7:1:5). It is believed that there was a strong hydrogen bonding interactions between the CNs that couldn't overcome the interactions between DMF and nanocrystals, which resulted in the agglomeration of nanocrystals in suspension and eventually inside the fibers. This agglomeration of nanocrystals in the fibers will decrease crystallinity of the PLA fiber matrix at some extent. However for the nanocomposites with lower content of CNs higher crystallinity values were obtained due to less interaction of hydrogen bonds and better dispersion along the fibers.

3.7 Cyto-compatibility Study of Nanocomposites

One of the main goals of this project is to determine whether or not the nanocomposites prepared are cyto-compatible to be potentially used as scaffolds in BTE. It has been found that PLA is a cyto-compatible polymer widely used in tissue engineering. HA is one of the main constituents of natural bone and the addition of it to synthetic scaffolds usually improves cell adhesion and proliferation. However, as to our knowledge, the evaluation of CNs as cytocompatible materials has not been reported. In the following study we were able to culture cells for one week on the pure PLA and on the highest and lowest CNs content nanocomposites prepared. Three dimensional images were taken by confocal microscopy. In Figure we can see a mixture of live (green) and dead (red) cells on the control (PLA) nanocomposite scaffolds. However, with the incorporation of CNs into the fibers we were able to improve cytocompatibility of the scaffolds (Figures 75 to 79). For the lowest content of CNs we can still see red staining from dead cells, but it can still be

seen more cells alive than in the PLA nanocomposite scaffold. For the highest content of CNs we can see better confluency of cells; no red staining of dead cells and more oriented growth along the fibers (Figures 76 and 78).

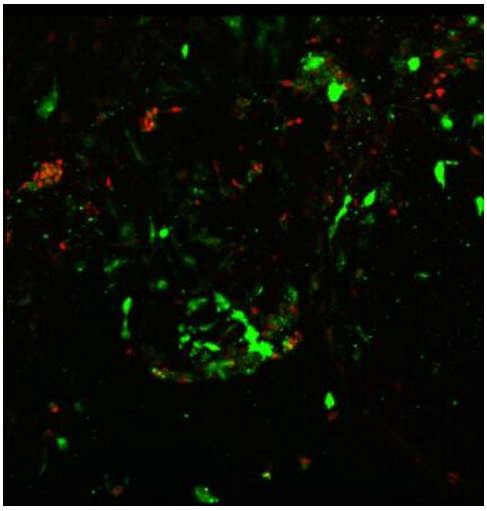

Figure75. AD-hMSCs cultured on pure PLA scaffold for 7 days

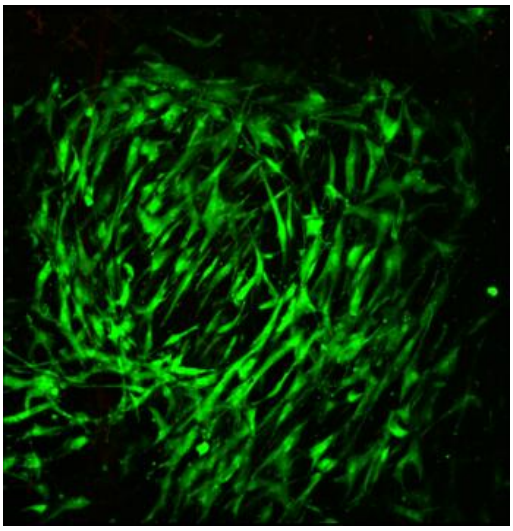

Figure76. AD-hMSCs cultured on PLA/CNs (7:1) nanocomposite scaffold for 7 days

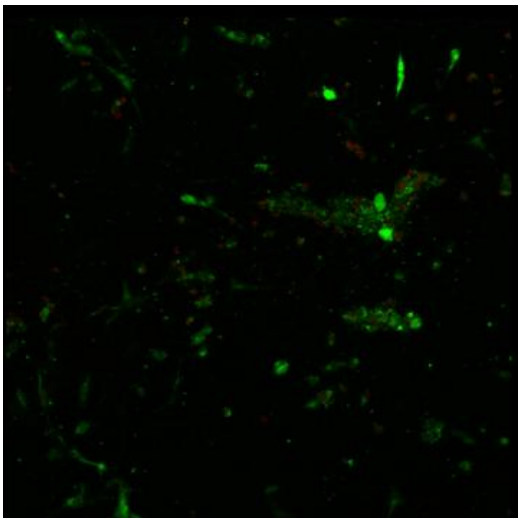

Figure77. AD-hMSCs cultured on PLA/CNs (17:1) nanocomposite scaffold for 7 days

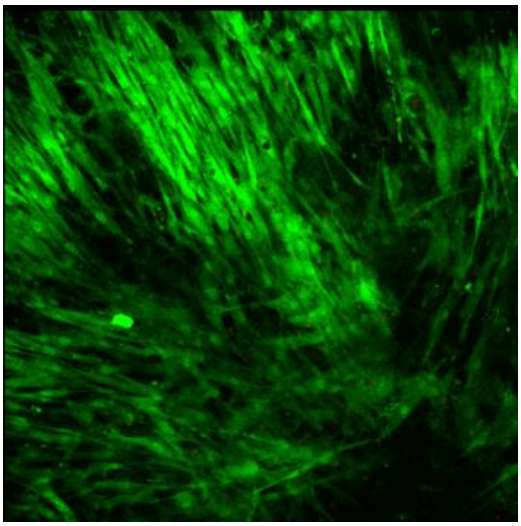

Figure78. AD-hMSCs cultured on PLA/CNs/HA (7:1:5) nanocomposite scaffold for 7 days

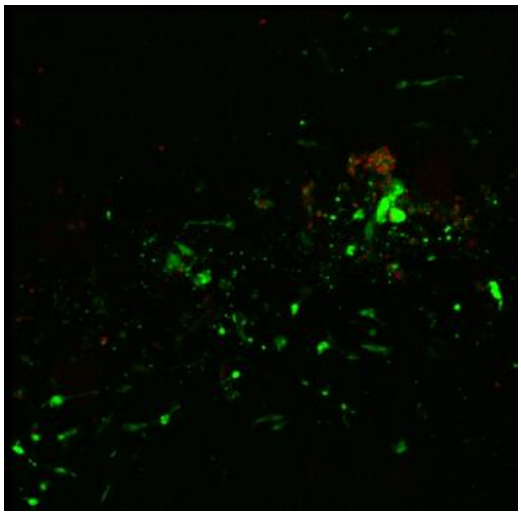

Figure 79. AD-hMSCs cultured on PLA/CNs/HA (17:1:5) nanocomposite scaffold for 7 days

Chapter 4

4.1 Conclusion

This project has shown the feasibility of the fabrication of a novel renewable PLA/CNs nanocomposite. The main goal of this project was to incorporate CNs into PLA fibers to reinforce PLA nanofiber matrix. Poly (lactic acid) / Cellulose Nanocrystals (PLA / CNs) were simultaneously electrospun to fabricate a nanocomposite scaffold. The results obtained from TGA and TEM confirm the presence of CNs in the fiber. Some fibers show an even dispersion of nanocrystals along the fiber; however some others show agglomeration of them. It is hypothesized that this agglomeration caused by hydrogen bonds interactions between the CN have caused a decrease in crystallinity of the polymer. It is clear that CNs reinforced the PLA fiber matrix as shown in the tensile strength results. However, the highest strength was not shown by the nanocomposite with the highest content of CNs which, may also be due to the CNs agglomeration. Life/Dead cell

viability assay was performed. Cells were alive up to 7 days for all the nanocomposite scaffolds. As we increased the content of nanocrystals in the fibers we saw a better confluency of cells, which is indicative of cytocompatibility of CNs. These results have demonstrated the feasibility of the fabricated PLA/CNs nanocomposite as a potential scaffold for bone tissue engineering.

4.2 Future Work

In order to further understand the nanocomposite properties it is useful to perform some other analyses.

- As shown in this work, crystallinity values obtained for the nanocomposites are not very well correlated. A possible approach to further understand this behavior is to use X-Ray diffraction technique and compare these results with the DSC results obtained in this work.
- It is also proposed the preparation of a thicker mat by increasing the concentration of PLA in solution. This approach will improve mechanical testing of the nanocomposites.
- To analyze viscosity and conductivity of the solution will be an useful approach in order to understand better solutions behavior during the electrospinning process. High conductivities and low viscosities will result in small fiber diameters.
- By preparing aligned fibers we are able to control cell alignment and improve mechanical properties. By increasing the speed of the rotating drum in the electrospinning apparatus we hypothesize that will result in fiber alignment.

- It is proposed to study pore distribution and pore size since this is of high importance for cell adhesion and proliferation. By increasing pore distribution and pore size we are able to allow a better cell adhesion and penetration into the fiber matrix.

References:

1. Shu, D. (2004). *Biomaterials and tissue engineering*. Germany: Springer. 195-243
2. Murugan, R.; Ramakrishna, S.; Design strategies of tissue engineerin/g scaffolds with controlled fiber orientation. *Tissue engineering*. 13 (8) **2007.** P. 1845-1866
3. Ryan. J. M.; Barry, F. P.; Murphy, J. M.; Mahon, B. P.; Mesenchymal stem cells avoid allogeneic rejection. *Journal of Inflammation*. 2 (8) **2005**. P. 1-11
4. Reis, R.; San Roman, J. (2005). 2. *Biodegradable systems in tissue engineering and regenerative medicine*. Florida: CRC press. 457-478
5. Dyson, J. A.; Genever, P. G.; Dalgarno, K. W.; Wood, D. J.; Development of custom-built bone scaffolds using mesenchymal stem cells and apatite-wollastonite glass-ceramics. *Tissue engineering*. 13 (12) **2007**. P. 2891-2901
6. Welter, J. F.; Solchaga, L. A.; Penick, K. J.; Simplification of aggregate culture of human mesenchymal stem cells as a chondrogenic screening assay. *BioTechniques.* 42 (6) **2007**. P. 732-737
7. Eglin, D.; Mortisen, D.; Alini, M.; Degradation of synthetic polymeric scaffolds for bone and cartilage tissue repairs. *Soft Matter*. 5 **2009**. P. 938-947
8. Xin, Z.; HaiLuo, F.; AiHua, Y.; DePing, W.; WenHai, H.; Ying, Z.; XinQuan, J.; In vitro bioactivity and cytocompatibility of porous scaffolds of bioactive borosilicates glasses. *Chinese Science Bulletin*. 54 (18) **2009**. P. 3180-3186
9. Park, J. B.; Bronzino, J. D. (2003). *Biomaterials Principles and Applications.* Florida: CRC Press LLC. 89
10. Hollister, S. J.; Porous scaffold design for tissue engineering. *Nature Materials*. 4 **2005**. P. 518-524

11. Sun, S.; Titushkin, I.; Cho, M.; Regulation of mesenchymal stem cell adhesion and orientation in 3D collagen scaffold by electrical stimulus. *Bioelectrochemistry*. 69 **2006**. P. 133-141
12. Wang, W.; Itoh, S.; Konno, K.; Kikkawa, T.; Ichinose, S.; Sakai, K.; Ohkuma, T.; Watabe, K.; Effects of Schwann cell alignment along the oriented electrospun chitosan nanofibers on nerve regeneration. *Journal of Biomedical Materials Research Part A*. 91 (4) **2009**. P. 994-1005
13. Liu, X.; Ma, P. X.; Polymeric scaffolds for bone tissue engineering. *Annals of Biomedical Engineering*. 32 (3) **2004**. P. 477-486
14. Dersch, R.; Graeser, M.; Greiner, A.; Wendorff, J. H.; Electrospinning of nanofibres: towards new technique, functions, and applications. *Australian Journal of Chemistry*. 60 **2007**. P. 719-728
15. Sanchez-Garcia, M. D.; Gimenez, E.; Lagaron, J. M.; Morphology and barrier properties of solvent cast composites of thermoplastic biopolymers and purified cellulose fibers. *Carbohydrate Polymers*. 71 **2008**. P. 235-244
16. Han, S. O.; Son, W. K.; Park, W. H.; Electrospinning of ultrafine cellulose fibers and fabrication of poly(butylenes succinate) biocomposites reinforced by them. *Journal of Applied Polymer Science*. 107 **2008**. P. 1954-1959
17. http://www.denniskunkel.com/DK/Medical/26444B.html
18. Pan, H.; Li, L.; Hu, L.; Cui, X.; Continuous aligned polymer fibers produced by a modified electrospinning method. *Polymer*. 47 **2006**. P. 4901-4904

19. De Vrieze, A.; Westbroek, P.; Van Camp, T.; Van Langenhove, L.; Electrospinning of chitosan nanofibrous structures: feasibility study. *Journal of Materials Science*. 42 (19) **2007**. P. 8029-8034.
20. Kulpinski, P.; Cellulose nanofibers prepared by N-methylmorpholine-N-oxide method. *Journal of Applied Polymer Science*. 98 **2005**. P. 1855-1859
21. Theron, S. A.; Zussman, E.; Yarin, A. L.; Experimental investigation of the governing parameters in the electrospinning of polymer solutions. *Polymer*. 45 **2004**. P. 2017-2030
22. Dong, C.; Yuan, X.; He, M.; Yao, K.; Preparation of PVA/PEI ultra-fine fibers and their composite membrane with PLA by electrospinning. *Journal of Biomaterial Science*. 17 (6) **2006**. P. 631-643
23. Jeong, S. I.; Ko, E. K.; Yum, J.; Jung, C. H.; Lee, Y. M.; Shin, H.; Nanofibrous poly(lactic acid)/hydroxyapatite composite scaffolds for guided tissue regeneration. *Macromolecular Bioscience*. 8 **2008**. P. 328-338
24. Hsu, C. M.; Shivkumar, S.; N,N-dimethylformamide additions to the solution for the electrospinning of poly(caprolactone) nanofibers. *Macromolecular Materials and Engineering*. 289 **2004**. P. 334-340
25. Kwon, I. K.; Kidoaki, S.; Matsuda, T.; Electrospun nano-to fiber fabrics made of biodegradable copolyesters: structural characteristics, mechanical properties and cell adhesion potential. *Biomaterials*. 26 **2005**. P. 3929-3939
26. Yoshimoto, H.; Shin, Y. M.; Terai, H.; Vacanti, J. P.; A biodegradable nanofiber scaffold by electrospinning and its potential for bone tissue engineering. *Biomaterials*. 24 **2003**. P. 2077-2082

27. Park, J. Y.; Lee, I. H.; Bea, G. N.; Optimization of the electrospinning conditions for preparation of nanofibers from polyvinylacetate (PVAc) in ethanol solvent. *Journal of Industrial and Engineering Chemistry*. 14 (6) **2008**. P. 707-713

28. Badami, A. S.; Kreke, M. R.; Thompson, M. S.; Riffle, J. S.; Goldstein, A. S.; Effect of fiber diameter on spreading, proliferation, and differentiation of osteoblastic cells on electrospun poly(lactic acid) substrates. *Biomaterials*. 27 **2006**. P. 596-606

29. McCullen, S. D.; Stano, K. L.; Stevens, D. R.; Roberts, W. A.; Monteiro-Riviere, N. A.; Clarke, L. I.; Gorga, R. E.; Development, optimization, and characterization of electrospun poly(lactic acid) nanofibers containing multi-walled carbon nanotubes. *Journal of Applied Polymer Science*. 105 **2007**. P. 1668-1678

30. Jun, Z.; Hou, H.; Schaper, A.; Wendorff, J. H.; Greiner, A.; Poly-l-lactide nanofibers by electrospinning- Influence of solution viscosity and electrical conductivity on fiber diameter and fiber morphology. *E-Polymers*. 9 **2003**. P. 1-9

31. Son, W. K.; Youk, J. H.; Lee, T. S.; Park, W. H.; The effects of solution properties and polyelectrolyte on electrospinning of ultrafine poly(ethylene oxide) fibers. *Polymer*. 45 **2004**. P. 2959-2966

32. Magalhaes, W. L.; Cao, X.; Lucia, L.A.;Cellulose nanocrystals/cellulose core-in-shell nanocomposite assemblies. *Langmuir*. 25 (22) **2009**. P. 13250-13257

33. Lucia, L., Rojas, O. (2009). *The Nanoscience and Technology of Renewable Biomaterials*. Wiley. 294-314

34. Rogel, M.R.; Qiu, H.; Ameer, G.A.; The role of nanocomposites in bone regeneration. *Journal of Materials Chemistry*. 18 **2008.** P. 4233-4241
35. Burr, D.B.; The contribution of the organic matrix to bone's material properties. *Bone*. 31 (1) **2002**. P. 8-11
36. Gupta, H.S.; Zioupos, P.; Fracture of bone tissue: The hows' and the whys'. *Medical Engineering & Physics*. 30 **2008.** P. 1209-1226
37. Giannoudis, P., Dinopoulos, H., Tsiridis, E.; Bone substitutes: An update. *Injury: International Journal of the Care of the Injured.* 36S **2005.** P. S20-S27
38. http://www.aaos.org/research/stats/patientstats.asp
39. Parikh, S.; Bone graft substitutes: Past, Present, Future. *Journal of Postgraduate Medicine*. 48 **2002.** P. 142-148
40. Kroeze, R.J.; Helder, M.N.; Govaert, L.E.; Smit, T.H.; Biodegradable Polymers in Bone Tissue Engineering. *Materials*. 2 **2009**. P. 833-856
41. Alvarez, K.; Nakajima, H.; Metallic scaffolds for bone regeneration. *Materials*. 2 **2009**. P. 790-832
42. Stevens, M.M.; Biomaterials for bone tissue engineering. *Materials today*. 11 (5) **2008**. P. 18-25
43. Kamynina, O.K.; Gotman, I.; Gutmanas, E.; Sytschev, A. E.; Vadchenko, S.G.; Balikhina, E.N.; Combustion synthesis of porous Ti-Co alloys for orthopedic applications. *International Journal of Self-Propagating High-Temperature Synthesis*. 18 (2) **2009**. P.102-108

44. Yoshikawa, H.; Tamai, N.; Murase, T.; Myoui, A.; Interconnected porous hydroxyapatite ceramics for bone tissue engineering. *Journal of the Royal Society Interface*. 6 **2009**. P. S341-S348

45. Zhang, L.; Ramsaywack, S.; Fenniri, H.; Webster, T.J.; Osteoblast behaviors on novel self-assembled helical rosette nanotubes and hydrogel composites for bone tissue engineering. *Materials Research Society*. 1056 **2008**. P

46. Verma, D.; Bhowmik, R.; Mohanty, B.; Katti, D.R.; Katti, K.; Role of interfacial interactions on mechanical properties of biomimetic composites for bone tissue engineering. *Materials Research Society*. 896E **2006**. P. 0898-L08-03.1-0898-L08-03.6

47. Karlsson, K.H.; Hupa, L.; Thirty-five years of guided tissue engineering. *Journal of non-crystalline solids*. 354 **2008.** P. 717-721

48. Wuisman, P.I.; Smit, T.H.; Bioresorbable polymers: heading for a new generation of spinal cages. *European Spine Journal*. 15 **2006**. P. 133-138

49. Sabir, M. I.; Xu, X.; Li, L.; A review on biodegradable polymeric materials for bone tissue engineering applications. *Journal of materials science*. 44 **2009**. P. 5713-5724

50. Glasscock, David; Atolino, Walter; Kozielski, Gary; Martens, Marv. "High performance polyamides fulfill demanding requirements for automotive thermal management components." Dupont. 2010. Web. 17 Mar. 2010.

51. Galeski, A.; Strength and thoughness of crystalline polymer systems. *Progress in Polymer Science*. 112 **2003**. P. 1643-1699

52. Buschle-Diller, G.; Hawkins, A.; Copper, J.; (2006). *Modified Fibers with Medical and Specialty Applications*. Springer Netherlands. 67-80

53. Sabir, M. I.; Xu, X.; Li, L.; A review on biodegradable polymeric materials for bone tissue engineering applications. *Journal of materials science*. 44 **2009**. P. 5713-5724

54. Xu, X.; Yang, Q.; Wang, Y.; Yu, H.; Chen, X.; Jing, X.; Biodegradable electrospun poly(lactide) fibers containing antibacterial silver nanoparticles. *European Polymer Journal*. 42 **2006**. P. 2081-2087

55. Li, D.; Frey, M. W.; Vynias, D.; Baeumner, A. J.; Availability of biotin incorporated in electrospun PLA fibers for streptavidin binding. *Polymer*. 48 **2007**. P. 6340- 6347

56. Chen, J.; Chu, B.; Hsiao, B. S.; Mineralization of hydroxyapatite in electrospun nanofibrous poly(L-lactic acid) scaffolds. *Journal of biomedical materials research part A.* 79a (2) **2006**. P 307-317

57. Kumbar, S. G.; Nukavarapu, S. P.; James, R.; Nair, L. S.; Laurencin, C. T.; Electrospun poly(lactic acid-co-glycolic acid) scaffolds for skin tissue engineering. *Biomaterials*. 29 **2008**. P. 4100-4107

58. Dong, C.; Yuan, X.; He, M.; Yao, K.; Preparation of PVA/PEI ultra-fine fibers and their composite membrane with PLA by electrospinning. *Journal of Biomaterial Science, Polymer Edition*. 17 (6) **2006**. P. 631-643

59. Kim, H. W.; Lee, H. H.; Knowles, J. C.; Electrospinning biomedical nanocomposite fibers of hydroxyapatite/poly(lactic acid) for bone regeneration. *Journal of biomedical materials research part A.* 79a (3) **2006**. P. 643-649

60. Luu, Y. K.; Hsiao, B. S.; Chu, B.; Hadjiargyrou, M.; Development of nanostructured DNA delivery scaffold via electrospinning of PLGA and PLA-PEG block copolymers. *Journal of controlled release*. 89 **2003**. P. 341-353
61. Park, C.H.; Hong, E.Y.; Kang, Y.K.; Effects of spinning speed and heat treatment on the mechanical properties and biodegradability of polylactic acid fibers. *Journal of applied polymer science*. 103 **2007**. P. 3099-3104
62. Park, J. B.; Lakes, R. S. (2007). Biomaterials. New York: Springer New York. 485-515
63. Gupta, B.; Revagade, N.; Hilborn, J.; Poly(lactic acid) fiber: An overview. *Progress in Polymer Science*. 32 **2007**. P. 455-482
64. Ikada, Y.; Tsuji, H.; Biodegradable polyesters for medical and ecological applications. *Macromolecular Rapid Communications*. 21 **2000**. P. 117-132
65. Luu,Y. K.; Kim, K.; Hsiao, B. S.; Chu, B.; Hadjiargyrou, M.; Development of a nanostructured DNA delivery scaffold via electrospinning of PLGA and PLA-PEG block copolymers. *Journal of Controlled Release*. 89 **2003**. P. 341-353
66. Wang, Z.; Hou, X.; Mao, Z.; Ye, R.; Mo, Y.; Finlow, D. E.; Synthesis and characterization of biodegradable poly(lactic acid-co-glycine) via direct melt copolymerization. *Iranian Polymer Journal*. 17 (10) **2008**. P. 791-798
67. Barrera, D. A.; Zylstra, E.; Lansbury, P. T.; Langer, R.; Copolymerization and Degradation of Poly(lactic acid-co-lysine). *Macromolecules*. 28 **1995**. P. 425-432
68. Xin, X.; Hussain, M.; Mao, J. J.; Continuing differentiation of human mesenchymal stem cells and induced chondrogenic and osteogenic lineages in electrospun PLGA nanofiber scaffold. *Biomaterials*. 28 **2007**. P. 316-325

69. Mendenhall, J.; Li, D.; Frey, M.; Hinestroza, J.; Babalola, O.; Bonnasar, L.; Batt, C. A.; Piezoelectric poly(3-hydroxybutyrate)-poly(lactic acid) three dimensional scaffolds for bone tissue engineering. *Materials Research Society*. 1025 **2008**. P. 1025-B12-03

70. Ko, E. K.; Jeong, S. I.; Rim, N. G.; Lee, Y. M.; Shin, H.; Lee, B.; In vitro osteogenic differentiation of human mesenchymal stem cells and in vivo bone formation in composite nanofiber meshes. *Tissue Engineering: Part A*. 14(12) **2008**. P. 2105-2119

71. Xu, X.; Yang, Q.; Wang, Y.; Yu, H.; Chen, X.; Jing, X.; Biodegradable electrospun poly(lactide) fibers containing antibacterial silver nanoparticles. *European Polymer Journal*. 42 **2006**. P. 2081-2087

72. Li, D.; Fey, M.; Vynias, D.; Baeumner, A. J.; Availability of biotin incorporated in electrospun PLA fibers for streptavidin binding. *Polymer*. 48 **2007**. P. 6340-6347

73. Kim, H. W.; Yu, H. S.; Lee, H. H.; Nanofibrous matrices of poly(lactic acid) and gelatin polymeric blends for the improvement of cellular responses. *Journal of Biomedical Materials Research Part A*. 87(1) **2008**. P. 25-32

74. Ramos, L. P.; The chemistry involved in the steam treatment of lignocellulosic materials. *Quimica Nova*. 26(6) **2003**. P. 863-871

75. Kvien, I.; Tanem, B. S.; Oksman, K.; Characterization of cellulose whiskers and their nanocomposites by atomic force and electron microscopy. *Biomacromolecules*. 6 **2005**. P. 3160-3165

76. Lu, Y.; Weng, L.; Cao, X.; Biocomposites of plasticized starch reinforced with cellulose crystallites from cottonseed linter. *Macromolecular Bioscience*. 5 **2005**. P. 1101-1107

77. Van den Berg, O.; Capadona, J. R.; Weder, C.; Preparation of homogeneous dispersion of tunicate cellulose whiskers in organic solvents. *Biomacromolecules*. 8 **2007**. P. 1353-1357

78. Samir, M. A.; Alloin, F.; Sanchez, J. Y.; El Kissi, N.; Dufresne, A.; Preparation of cellulose whiskers reinforced nanocomposites from an organic medium suspension. *Macromolecules*. 37 **2004**. P. 1386-1393

79. Goussé, C.; Chanzy, H.; Excoffier, G.; Soubeyrand, L.; Fleury, E.; Stable suspensions of partially silylated cellulose whiskers dispersed in organic solvents. *Polymer*. 43 **2002**. P. 2645-2651

80. Viet, D.; Beck, S. C.; Gray, D. G.; Dispersion of cellulose nanocrystals in polar organic solvents. *Cellulose*. 14 **2007**. P. 109-113

81. Helenius, G.; Backdahl, H.; Bodin, A.; Nannmark, U.; Gatenholm, P.; Risberg, B.; In vivo biocompatibility of bacterial cellulose. *Journal of Biomedical Materials Research Part A.* 76 A (2) **2005**. P. 431-438

82. Muller, F. A.; Muller, L.; Hofmann, I.; Greil, P.; Wenzel, M. M.; Staudenmaier, R.; Cellulose based scaffold materials for cartilage tissue engineering. *Biomaterials*. 27 **2006**. P. 3955-3963

83. Goldstein, J.; Newbury, D.; Joy, D.; Lyman, C.; Echlin, P.; Lifshin, E.; Sawyer, L.; Michael, J. (2003) Scanning electron microscopy and x-ray microanalysis. New York: Springer New York.

84. Schweitzer, Jim. “Scanning Electron Microscopy.” Purdue University. 6 Oct. 2006. Web. 17 Mar. 2010.
85. McCulloch, Dougal. “Electron Microscopy- Introduction, The Transmission Electron Microscope (TEM), The Scanning Electron Microscope (SEM), Elemental Identification.” RMIT University. 2010. Web. 17 Mar. 2010.
86. “Hitachi HF2000 Transmission Electron Microscope.”Analytical Instrumentation Facilities. North Carolina State University. 22 Jan. 2008. Web. 17 Mar. 2010.
87. “Transmission Electron Microscopy” Biovisionz. n.d. Web. 17 Mar. 2010.
88. “Introduction to Fourier Transform Infrared Spectrometry.” Thermo Nicolet. 2001. Web. 17 Mar. 2010.
89. Hubbe, M. “Mini-Encyclopedia of Papermaking Wet-End Chemistry.” North Carolina State University. n.d. Web. 17 Mar. 2010.
90. http://people.eku.edu/ritchisong/554images/Hydrophobic_hydrophilic2.jpg
91. Somasundaran, P. (2007) Encyclopedia of Surface and Colloidal Science. Boca Raton Florida: Taylor and Francis Group. P.1525-1527
92. Menard, K. P. (1999) Dynamic Mechanical Analysis: A Practical Introduction. Boca Raton Florida: CRC Press LLC. P.1-10
93. “Dynamic Mechanical Analysis.” Delsen Testing Laboratories Inc. 2009. Web. 17 Mar. 2010.
94. “Introduction to Dynamic Mechanical Analysis.” Anasys. n.d. Web. 17 Mar. 2010.
95. Menczel, J. D.; Prime, R. B. (2009) Thermal Analysis of Polymers. New Jersey: John Wiley & Sons Inc. P. 241

96. Hohne, G. W. H.; Hemminger, W. F.; Flammersheim, H. J. (2003) Differential Scanning Calorimetry. Germany: Springer-Verlag Berlin Heidelberg New York. P. 2-7

97. “Differential Scanning Calorimetry” Polymer Science Learning Center. University of Southern Mississippi. 1995-2005. Web. 17 Mar. 2010.

98. Wnek, G. E.; Bowlin, G. L. (2005). Encyclopedia of Biomaterials and Biomedical Engineering. New York: Informa Healthcare USA. P. 705-714